Tuberculosis 95 (2015) 95–111

Contents lists available at ScienceDirect

Tuberculosis

journal homepage: http://intl.elsevierhealth.com/journals/tube

REVIEW

Structural and functional features of enzymes of *Mycobacterium tuberculosis* peptidoglycan biosynthesis as targets for drug development

Gleiciane Leal Moraes [a], Guelber Cardoso Gomes [a, b], Paulo Robson Monteiro de Sousa [a], Cláudio Nahum Alves [a], Thavendran Govender [c], Hendrik G. Kruger [c, **], Glenn E.M. Maguire [c], Gyanu Lamichhane [d], Jerônimo Lameira [a, b, *]

[a] *Laboratório de Planejamento de Fármacos, Instituto de Ciências Exatas e Naturais, Universidade Federal do Pará, CEP 66075-110 Belém, PA, Brazil*
[b] *Instituto de Ciências Biológicas, Universidade Federal do Pará, CEP 66075-110 Belém, PA, Brazil*
[c] *Catalysis and Peptide Research Unit, School of Health Sciences, University of KwaZulu-Natal, South Africa*
[d] *Johns Hopkins University School of Medicine, Taskforce to Study Resistance Emergence & Antimicrobial Development Technology, 1503 E. Jefferson St, Baltimore, MD 21231, USA*

ARTICLE INFO

Article history:
Received 10 September 2014
Received in revised form
13 January 2015
Accepted 19 January 2015

Keywords:
TB
Homology modelling
Peptidoglycan
Drug design

SUMMARY

Tuberculosis (TB) is the second leading cause of human mortality from infectious diseases worldwide. The WHO reported 1.3 million deaths and 8.6 million new cases of TB in 2012. *Mycobacterium tuberculosis* (*M. tuberculosis*), the infectious bacteria that causes TB, is encapsulated by a thick and robust cell wall. The innermost segment of the cell wall is comprised of peptidoglycan, a layer that is required for survival and growth of the pathogen. Enzymes that catalyse biosynthesis of the peptidoglycan are essential and are therefore attractive targets for discovery of novel antibiotics as humans lack similar enzymes making it possible to selectively target bacteria only. In this paper, we have reviewed the structures and functions of enzymes GlmS, GlmM, GlmU, MurA, MurB, MurC, MurD, MurE and MurF from *M. tuberculosis* that are involved in peptidoglycan biosynthesis. In addition, we report homology modelled 3D structures of those key enzymes from *M. tuberculosis* of which the structures are still unknown. We demonstrated that natural substrates can be successfully docked into the active sites of the GlmS and GlmU respectively. It is therefore expected that the models and the data provided herein will facilitate translational research to develop new drugs to treat TB.

1. Introduction

In 2012, an estimated 8.6 million people developed TB and 1.3 million died from the disease (including 320,000 deaths among HIV-positive people) [1]. The peptidoglycan layer provides shape and rigidity and is essential for growth and survival of *Mycobacterium tuberculosis*. It is a polymer consisting of sugars and amino acids that forms a homogeneous layer exterior to the plasma membrane of eubacteria [2]. Peptidoglycan is a major component of the cell wall of almost all eubacteria. Structurally it consists of linear glycan chains with alternating units of *N*-acetylglucosamine (GlcNAc) and *N*-acetylmuramic acid (MurNAc), cross-linked by trans peptide bridges [3]. Since it is unique to bacterial cells, the enzymes that catalyse its biosynthesis offer an attractive target for discovery of new antibiotics against TB. In addition, the enzymes that constitute the peptidoglycan biosynthesis pathway in *M. tuberculosis* are essential and therefore their inhibition is expected to result in targeted killing of this pathogen [4].

The arrangement of genes responsible for peptidoglycan biosynthesis in *M. tuberculosis* is similar to that in other bacteria [5], likewise the biochemistry it displays [6]. The biosynthesis of peptidoglycan is a complex process that involves several reactions in different cytoplasmic and membranes steps [7]. Stage one occurs in the cytosol and can be divided into four sets of reactions: (1) formation of UDP-GlcNAc from fructose-6-phosphate, (2)

* Corresponding author. Laboratório de Planejamento de Fármacos, Instituto de Ciências Exatas e Naturais, Universidade Federal do Pará, CEP 66075-110 Belém, PA, Brazil.
** Corresponding author.
E-mail address: lameira@ufpa.br (J. Lameira).

http://dx.doi.org/10.1016/j.tube.2015.01.006
1472-9792/

formation of UDP-MurNAc from UDP-GlcNAc, (3) assembly of the peptide stem leading to UDP-MurNAc-tetrapeptide or UDP-MurNAc-pentapeptide and (4) 'side' or 'annex' pathways of synthesis of D-glutamic acid and the dipeptide D-alanyl-D-alanine (Figure 1) [2]. Despite the importance of the cytoplasmic step for biosynthesis of peptidoglycan in *M. tuberculosis*, the 3D structures of the enzymes involved therein have not been solved yet. The second stage of the synthesis occurs in the membrane where the disaccharide-peptide monomer units are assembled and polymerized [8]. The membrane steps are assembly and polymerization of the disaccharide-peptide monomer unit and are beyond the scope of this study.

Homology modelling [9] is a tool that can be used to generate reasonable protein structures by providing a 3D model from a template protein primary sequence based on the structures of one or more homologous proteins (>25% homology) of which the 3D structure(s) have been reported. Recently, we have used homology modelling to determine 3D structure of the regulatory response protein (PhoP) of *Corynebacterium pseudotuberculosis* [10], sialidases from *Trypanosoma brucei* and *Trypanosoma evansi* [11] and O-glycoprotein 2-acetamino-2-deoxy-β-D-glucopyranosidase [12]. Herein, we have used homology modelling [9] to describe the 3D structure of the enzymes involved in cytoplasmic steps of biosynthesis of peptidoglycan, namely GlmS, GlmM, GlmU, MurA, MurB, MurC, MurD, MurE and MurF. Furthermore, we have also provided detailed information about the functions of these enzymes.

2. Methods

Homology modelling allows the construction of the tertiary structure of a protein based on the primary structure similarity [9]. This technique is only possible because the 3D structures of homologous proteins are conserved during the evolutionary process especially functional residues, since preserving the structure is

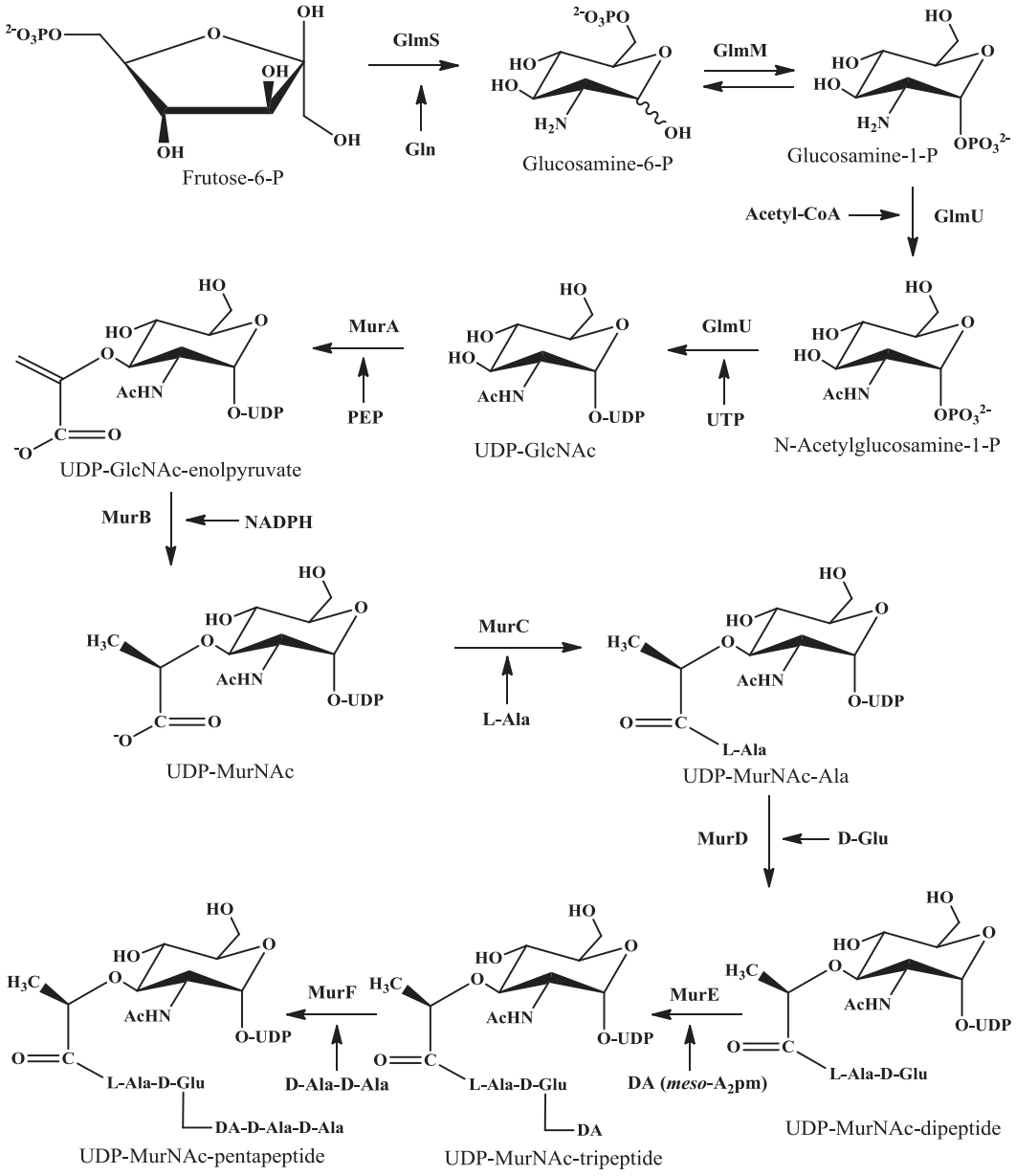

Figure 1. The cytoplasmic steps of peptidoglycan biosynthesis. Diamino acid (DA), *meso*-A_2pm (2,6-diaminopimelic acid) or L-Lys.

crucial to the maintenance and performance of specific functions [9]. In order to evaluate if the models obtained in this study could provide insight to design of new potential inhibitors, we have used the molecular docking technique to dock the substrate D-fructose-6-phosphate (Fru6P) and uridine-diphospho-N-acetylglucosamine (UDP-GlcNAc) to the active sites of the GlmS and GlmU respectively. It should be noted that docking results without a supportive method could be meaningless [13]. In this case we chose known X-ray structures of similar enzymes complexed to natural substrates as benchmark. The specific details about the setting of the homology modelling and molecular docking are provided with the Supporting information.

2.1. Modeling enzymes involved in biosynthesis of uridine-diphospho-N-acetylglucosamine

The uridine-diphospho-N-acetylglucosamine (UDP-GlcNAc) is an essential structural building block of the bacterial peptidoglycan, the lipopolysaccharide of Gram-negative bacteria, chitin, and mannoproteins of the fungal cell wall [14]. In bacteria, UDP-GlcNAc biosynthesis from fructose-6-phosphate comprises four successive reactions catalysed by three different enzymes [15]. The entry substrate, fructose-6-phosphate (Fru6P), is converted to glucosamine-6-phosphate (GlcN6P) by glucosamine-6-phosphate synthase (GlmS). Subsequently, the isomerisation of glucosamine-6-phosphate to glucosamine-1-phosphate (GlcN1P) is processed by phosphoglucosamine mutase (GlmM). The last two steps of the reaction involve the acetyltransfer and uridyltransfer during the transformation of GlcN1P to UDP-GlcNAc. This double reaction is catalysed by the bifunctional enzyme N-acetylglucosamine-1-phosphate uridyltransferase (GlmU), which has acetyltransferase and uridyltransferase activity [2]. In this first section, we describe the 3D structures of GlmS, GlmM and GlmU enzymes. Also, we show the catalytic mechanisms involving these enzymes that lead to UDP-GlcNAc biosynthesis. Finally, details about the results of Homology modelling and evaluations of the structure models are provided with the Supplementary material.

2.2. GlmS

Glucosamine-6-phosphate synthase (GlmS) is a dimeric enzyme that belongs to the family of glutamine-dependent amidotransferases, which catalyses the conversion of D-fructose-6-phosphate (Fru6P) into D-glucosamine-6-phosphate (GlcN6P) in the first step of pathway for the formation of UDP-GlcNAc [14]. This is a key point in the metabolic control of the biosynthesis of amino sugar-containing macromolecules. Depending on its prokaryotic, lower or higher eukaryotic origin, GlcN6P synthases have been termed GlmS, Gfa or Gfat. In mammalian cells, the equivalent protein (Gfat) is a tetrameric enzyme. It has attracted significant attention because of the observation that the hexosamine biosynthetic pathway in humans where this enzyme functions, acts as a glucose sensor and it is a mediator of insulin resistance with crucial implications in the vascular complications of type II diabetes [16,17]. *Escherichia coli* and *Candida albicans* GlmS enzymes have been reviewed [18,19]. Among GlcN6P synthases, the *E. coli* enzyme (GlmS) is the best characterized protein. It functions as a homodimer, each monomer is composed of two structurally and functionally distinct domains. The N-terminal glutaminase domain (residues 1–239) of 27 kDa hydrolyses glutamine to glutamate and ammonia, whereas the C-terminal synthase domain (residues 249–608) of 40 kDa binds the nitrogen acceptor and uses the ammonia that is produced for the conversion offructose-6-phosphate into glucosamine-6-phosphate [20].

The glutamine hydrolysis reaction of GlmS (*E. coli*) uses the cysteine thiol of this enzyme (Cys1), which forms a γ-glutamyl thioester intermediate (Figure 2A). The N-terminal group of Cys1 activates the thiol group *via* a water molecule for nucleophilic attack on the carboxamide group of glutamine, producing an oxyanion tetrahedral intermediate stabilized by Nδ2of Asn98 and the NH group of Gly99. There after the oxyanion tetrahedral intermediate breaks down to yield γ-glutamylthioester and ammonia. Further hydrolysis proceeds through the oxyanion, producing glutamate and free enzyme [21]. The catalytic mechanism at the synthase domain (Figure 2B) begins with the Fru6P sugar ring opening facilitated by His504. This is followed by the formation of a Schiff base between Lys603 and the carbonyl group of Fru6P. The synthase binding site consists mostly of the C-tail and the His-loop in GlmS [14]. Transamination with ammonia from the glutaminase site (Figure 2A) yields fructosimine-6P. Glu488 is the likely base that deprotonates C1 of Fru6P producing the *cis*-enolamine and Lys485 is proposed to deprotonate the O5 hydroxyl group with simultaneous protonation of the C2 sp^2 carbon from Glu488 yielding the linear form of glucosamine-6P. Ring closure of the latter is facilitated by His504 (Figure 2) [22,23]. The catalytic mechanism and the key residues involved in this step are shown in Figure 2A and B.

Based on alignment of the amino acid sequences all catalytic residues are conserved in GlmS *M. tuberculosis* model obtained by homology modelling (Figure 3).

The GlmS is inhibited by glutamine analogues that may be either naturally occurring or synthetic in origin. Among the naturally occurring compounds, there is anticapsin [22], azaserine and albizziin [25]. One of the best known synthetic inhibitors of GlmS is 2-amino-2-deoxy-D-glucitol-6P ($IC_{50} = 56$ μM) [26]. The glutamine analogue 6-diazo-5-oxo-L-norleucine (DON) is known to irreversibly alkylate the thiol group of the N-terminal cysteine (Cis1). The following nucleophilic attack of the thiolate group on the diazonium group of the inhibitor leads to alkylation of the enzyme, which mimics the glutamyl-thioester intermediate formed during glutamine hydrolysis [27]. X-ray structure of the glutaminase domain of *E. coli* (PDB code: 1XFG) were solved in the presence of Glu-hydroxamate, a competitive inhibitor of the glutaminase site [28], and structures of the synthase domain in the presence of the GlcN6P product, D-glucose-6P (Glc6P, the product of the reaction in the absence of glutamine), and 2-amino-deoxyglucitol-6P, an analogue of a reaction intermediate, which is a competitive inhibitor of the synthase site [29]. Furthermore, trapping experiments demonstrated the formation of a Schiff base between Lys603 and pyridoxal 5′-phosphate, a competitive inhibitor of Fru6P [14].

2.3. GlmM

Phosphoglucosamine mutase (GlmM) catalyses the second of four successive steps, leading to the synthesis of UDP-GlcNAc from fructose-6-phosphate. This isomerase enzyme catalyses the interconversion of glucosamine-6-phosphate (GlcN6P) to glucosamine-1-phosphate (GlcN1P) [7]. Phosphoglucosamine mutases exist in various bacteria, including *Helicobacter pylori*, *Staphylococcus aureus*, *Pseudomonas aeruginosa*, *Streptococcus gordinii*, *Bacillus anthracis*, *Salmonella enterica serovar Typhimurium*, and *E. coli*; it has been characterized functionally and/or kinetically [30–37]. Mutations in GlmM appear to influence bacterial cell growth and morphology, biofilm formation, and sensitivity to penicillins [34].

The architecture of the four domains are demonstrated in the GlmM protein model [35]: Domain I (residues 1–159), domain II (residues 160–256), domain III (residues 257–371) and domain IV (residues 372–448) see Figure 4. All secondary structures in the template protein were conserved and the generated 3D structure

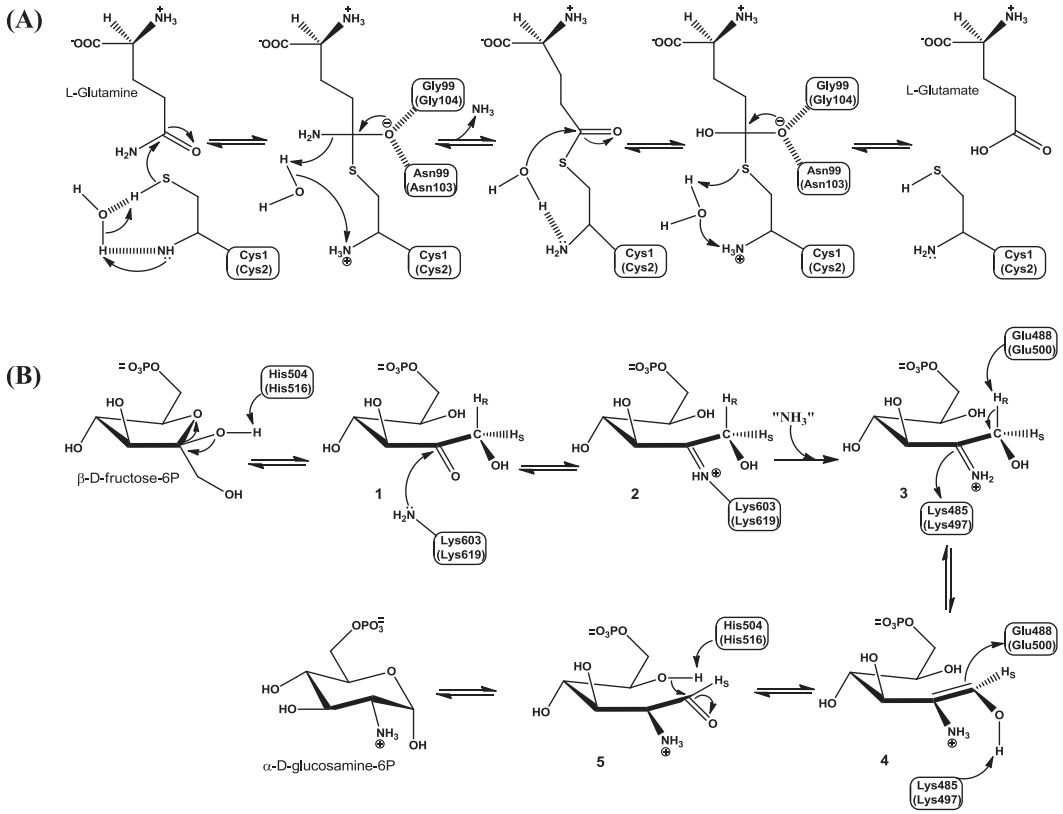

Figure 2. Reactions catalysed by GlmS. Catalytic mechanism at the synthase (A) and glutaminase (B) domain [21,24]. Catalytic residues of *M. tuberculosis* are shown in parenthesis.

is an acceptable model according to analysed parameters. Domains I to III share a fold, consisting of a mixed α/β core. The β-sheet of the core consists of four antiparallel β-strands. Each domain has α-helix between strands 1 to 2 and 2 to 3. Domain IV, by contrast, is topologically distinct, and consists of a 3-stranded, antiparallel β-sheet, flanked by two α-helices. A localization of the active site can be made on the basis of the position of the phosphoserine residue involved in phosphoryl transfer (in *M. tuberculosis* Ser102) at the approximate confluence of the four domains [36]. The 3D modelled structure of GlmM from *M. tuberculosis* is presented in Figure 4.

The presence of Mg^{2+} is required for full activity of GlmM, the phosphoserine residue in the active site is also required in the phosphoryl transfer reaction. Based on other enzymes in the phosphohexomutase family the active site of GlmM *M. tuberculosis* contains four key regions: (i) the phosphoserine residue involved in the phosphoryl transfer reaction, (ii) the metal-binding site, (iii) a sugar moiety of the substrate/product, and (iv) the phosphate binding site, which interacts with both substrate and the product [37].

The proposed reaction mechanism (Figure 5) requires two phosphoryl transfer reactions, first from the enzyme to substrate

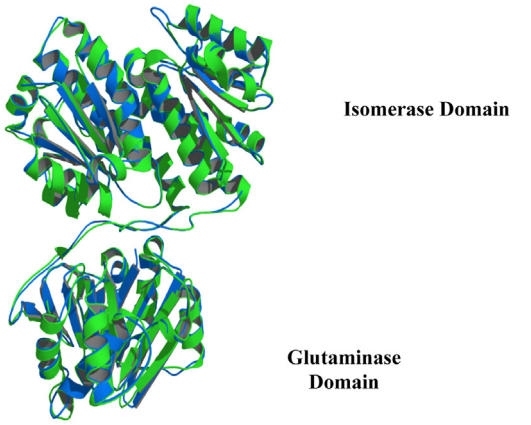

Figure 3. Superposition of the calculated GlmS protein of *M. tuberculosis* (blue) and *E. coli* (green) [21]. The 3D structure of the modelled enzyme is provided with the Supplementary material in PDB format. (For interpretation of the references to colour in this figure legend, the reader is referred to the web version of this article.)

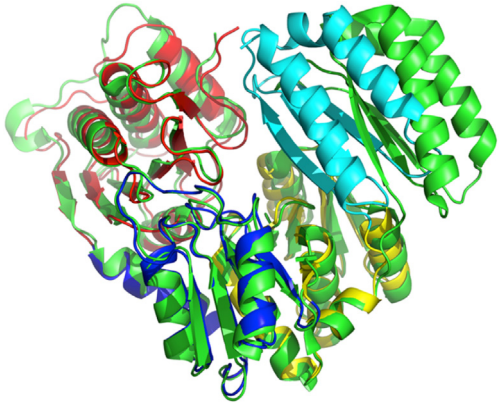

Figure 4. Superposition of the GlmM of *M. tuberculosis* and *B. anthracis* (green – 3PDK) [36], where domains I, II, III and IV are shown in red, blue, yellow and cyan, respectively. The 3D structure of the modelled enzyme is provided with the Supplementary material in PDB format. (For interpretation of the references to colour in this figure legend, the reader is referred to the web version of this article.)

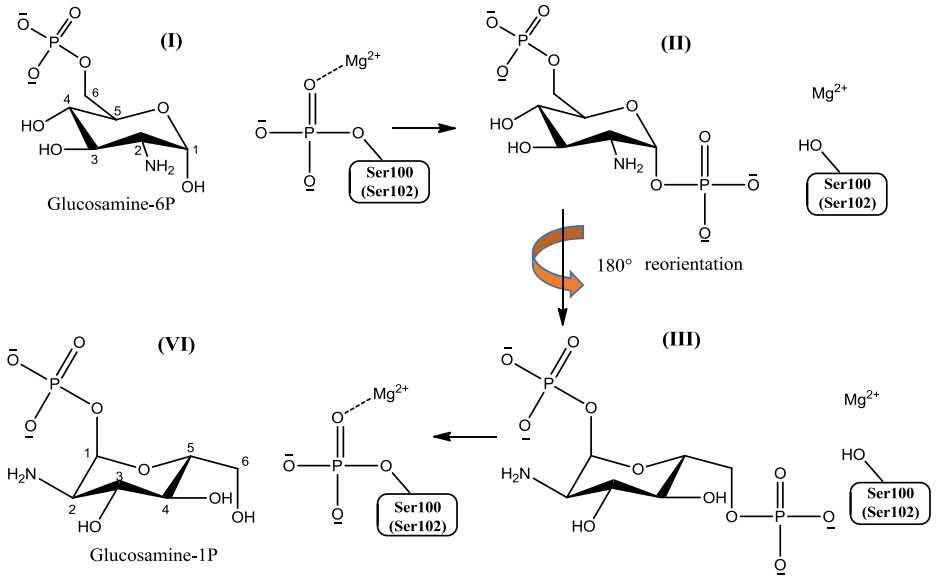

Figure 5. Reactions catalysed by GlmM [36]. Catalytic residues of *M. tuberculosis* in parenthesis.

and second from the reaction intermediate back to the enzyme. Based on alignment of amino acid sequences, Mehra-Chaudhary et al. (2011) [36] described the mechanism for *B. anthracis*. According to them the reaction is initiated by interaction with a general acid/base (Arg11), which abstracts a proton from the O1 or O6 hydroxyl of the phosphosugar and activates it for nucleophilic attack on phosphoserine 100. Initially the phosphorylated serine residue (Ser100) provides the phosphoryl group that is transferred to substrate creating a bisphosphorylated sugar intermediate (GlcN1,6diP). The phosphoryl oxygen (Oγ) of this residue also acts as a ligand for the metal ion (typically Mg^{2+}), while three other ligands for the metal are provided by the side chains of aspartate residues D240, D242, and D244. The metal serves to withdraw electrons from the leaving group, facilitating the phosphoryl transfer reaction. The side chains of the residues Glu325 and Ser327, present in a loop, interact with O3 and O4 hydroxyl groups of the phosphosugar substrate and product during the process. Residues involved in direct phosphate interaction include the side chains of Arg410, Ser412, and Arg419; the role of these residues is to stabilize the phosphate group of the substrate and product [37].

The GlmM enzyme exists in both phosphorylated and dephosphorylated forms *in vivo*, and the phosphorylated form reacts with either GlcN1P or GlcN6P but not with GlcN1,6diP. Steady-state kinetics characteristic of a ping-pong reaction suggest where GlcN1,6diP (*E. coli*) acts as the first product and second substrate [38]. Moreover the binding of the phosphosugar is associated with a hinge-type closure of domain IV, which reduces the volume and surface area of the active site cleft and positions the substrate for phosphoryl transfer [35].

2.4. GlmU

The bifunctional bacterial enzyme N-acetylglucosamine-1-phosphate uridyltransferase (GlmU) catalyses the last two steps of the formation of uridine-diphospho-N-acetylglucosamine (UDP-GlcNAc), an important precursor in bacterial peptidoglycan cell walls [2,39]. GlmU is responsible for two important biochemical activities in this process. The C-terminal acetyltransferase domain (residues 264–473) catalyses the transfer of an acetyl group from acetyl-CoA coenzyme to GlcN1P to produce N-acetylglucosamine-1-phosphate (GlcNAc1P), whereas the N-terminal uridyltransferase domain (residues 2–263) catalyses the transfer of uridine 5′-monophosphate from uridine 5′-triphosphate (UTP) to GlcNAc1P, in the presence of Mg^{2+} ions, yielding inorganic pyrophosphate and UDP-GlcNAc (Figure 6) [40]. In contrast to that, acetyltransfer of eukaryotic cells occurs on GlcN6P and not on GlcN1P and each step of the pathway is catalysed by a separate enzyme [2]. That makes this protein suitable for the potential design of non-toxic inhibitors. The 3D modelled structure of GlmU from *M. tuberculosis* is presented in Figure 6.

Dynamic light scattering and analytical gel filtration show that GlmU from *M. tuberculosis* is trimeric in solution [40] where each monomer consists of two distinct domains that are connected by a

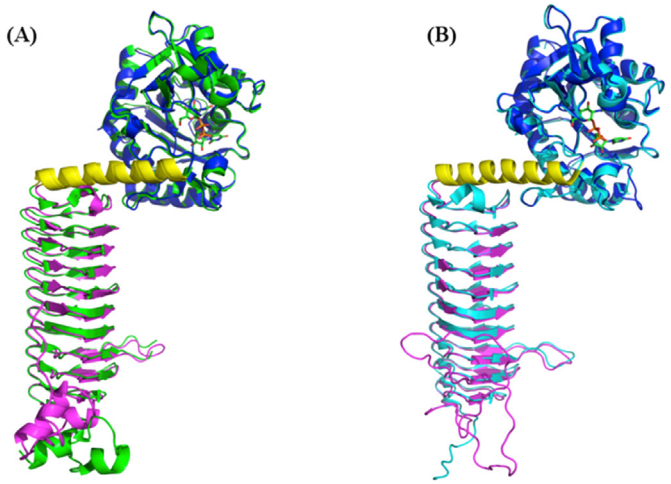

Figure 6. (A) Superposition of the GlmU modelled of *M. tuberculosis* (uridyltransferase and acetyltransferase domains are shown in blue and purple respectively) and 3D8V [40] crystal structure in complex with UDP-GlcNAc (green). The α-helical arm in yellow. (B) Superposition of the GlmU modelled of *M. tuberculosis* (uridyltransferase and acetyltransferase domains are shown in blue and purple respectively) and 1G97 [41] crystal structure in complex with UDP-GlcNAc (green). The α-helical arm in yellow. The 3D structure of the modelled enzyme is provided with the Supplementary material in PDB format. (For interpretation of the references to colour in this figure legend, the reader is referred to the web version of this article.)

long α-helical arm (Figure 6). The general mechanism for the GlmU catalysed reactions is presented in Figure 7.

The C-terminal acetyltransferase domain (residues 264–473) comprises ten repeats (ten coils) of about 18 residues, forming a regular left-handed parallel β-helix (LβH) structure and an extended C-terminal (≈30 amino acid residues) tailing as a disordered region. This extended region of the C-terminal is absent in the aforementioned orthologs. The deletion of the 30 amino acids results in complete loss of the acetyltransferase activity [42]. Each turn of acetyltransferase domain displays a triangular cross-section and is formed by three β-strands with a distinctive repetitive pattern of hydrophobic residues. Four sequential residues Asn397, Tyr398, Asp399 and Gly400 situated within turn 8 are highly conserved. These residues constitute a special insertion loop N-Y-D-G, which has been determined as a binding group of the sugar substrate in other species [43]. The residues directly involved in acetyl-CoA or CoA binding is positioned similarly in *E. coli*, *H. influenza* and *M. tuberculosis*. In the case of the *M. tuberculosis* GlmU, one of these residues is Trp460 [42]. In a recent study [43], 10 highly conserved residues within the C-terminal conserved region of *M. tuberculosis* GlmU were selected as mutation sites. These included Lys362, His374, Tyr398, Lys403, Ser416, Asn456, Glu458, Trp460, Arg463, and Ser474. In the LβH structure, the substitution of Lys362, His374, Tyr398 residues resulted in a reduction of approximately 90% acetyltransferase activity and rather lower affinity of GlmU acetyltransferase to both substrates, demonstrating that these three amino acids were possibly located in the active site for direct substrate recognition and binding in the catalysis of *M. tuberculosis* GlmU acetyltransferase [43]. Furthermore, Lys403 and Ser416 residues may play an important role in converting and releasing products, and for the Trp460 GlmU mutant, 97% of the acetyltransferase activity was lost and the affinity of Trp460 mutant to the two substrates was also completely undetectable [43].

The N-terminal of the Uridyltransferase domain (residues 2–264) has a typical uridyltransferase Rossmann fold (α/β-like fold). This active site can be divided into two substrate binding sites: (i) the uridine-binding region of UTP and the GlcNAc-binding region of GlcNAc1P. The substrate binding follows an ordered sequential (ii) mechanism in which UTP binding precedes GlcNAc1P binding, and a large conformational change occurs in the uridyltransferase active site upon formation of the GlmU complex with substrate GlcNAc1P, to form the UDP-GlcNAc product [45]. The uridine binding region consists of the following key residues in the UTP substrate recognition and catalysis process: The Ala13–Gly15, Arg19, Lys26, Gln83–Thr89, Asp114 and Glu166 structural segments form the uracyl and ribose binding subsites. The GlcNAc-binding site is comprised of the Thr89, Gly151, Asn181–Gly183, and Glu207–Thr211 structural segments that are arranged to recognize the N-acetylglucosamine moiety and to orchestrate structural rearrangements required to complete the uridyltransferase reaction [40,43].

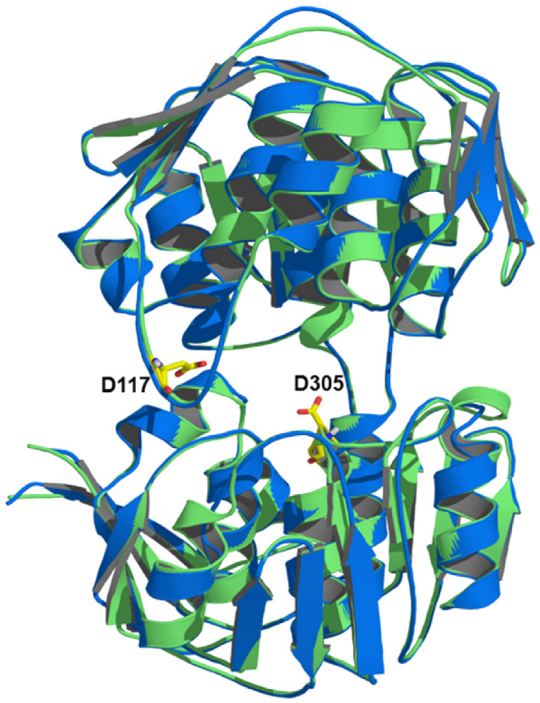

Figure 8. Superposition of the calculated MurA protein of *M. tuberculosis* (blue) and *H. influenzae* (green – 3SWE) [49]. Catalytic residues are shown. The 3D structure of the modelled enzyme is provided with the Supplementary material in PDB format. (For interpretation of the references to colour in this figure legend, the reader is referred to the web version of this article.)

Mochalkin and colleagues (2008) [46] proposed an inhibitor based on an allosteric mechanism, but it was not functional against Gram-positive bacteria. GlmU from these organisms contain naturally substitution of the Met or Leu for Glu224 (in *hi*GlmU) that are key residues in the interaction with inhibitors/substrates. Recently, electrophilic thiol-reactive molecules, such as maleimides and iodoacetamide, have been listed as inhibitors of the acetyltransferase domain [47,48]. Utilizing the assay developed by Pereira and colleagues [65], a total of 50,000 molecules were tested in duplicate for inhibition of GlmU, resulting in the identification of 63 molecules; 37 specific to the acetyltransferase activity of GlmU were selected for study. The potency and specificity of three identified small-molecule inhibitors (MAC0021939, MAC0008028 and MAC0029665) highlight them as excellent candidates for further study [45].

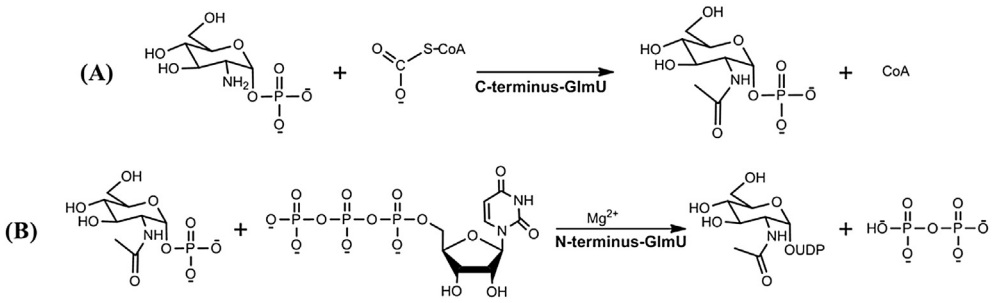

Figure 7. Reactions catalysed by GlmU [39]. Reaction at the acetyltransferase (A) [42,43] and pyrophosphorylase (B) [44].

2.5. Biosynthesis of UDP-N-acetylmuramic acid

Previously, we described the UDP-GlcNAc biosynthesis and structure of GlmS, GlmM and GlmU. In this section, we focus on the biosynthetic pathway that leads to formation of the monomeric building block N-acetylglucosamine-N-acetylmuramylpentapeptide *via* a six-step process catalysed by enzymes MurA, MurB, MurC, MurD, MurE and MurF, all of which are essential in *M. tuberculosis* [4]. The bacterial enzyme MurA and MurB are involved in the formation of UDPMurNAc (UDP-N-acetylmuramic acid) from UDP-GlcNAc, which occurs in two steps.

2.6. MurA

UDP-*N*-acetylglucosamine 1-carboxyvinyltransferase (MurA) contains 418 amino acid residues in two domains. Each domain consists of six helices and three four-stranded β sheets. The N- and C-terminals are located in domain I and II, but domain I (residues 232–418 and 1–18) consists mainly of the C-terminal portion whereas the N-terminal portion of the sequence resides largely in domain II (residues 22–228). One striking feature of the MurA structure is the six fold repetition of one folding unit or subdomain consisting of a β1, α1, β2, α2, β3 and β4 cores. Each domain contains three folding units. The domains are linked by two strands each of 3 and 4 amino acids in length, respectively (residues 19–21 and 229–232) (Figure 8).

The reaction catalysed by MurA proceeds *via* an addition–elimination mechanism. This reaction is mechanistically unusual as it involves the attack at the electrophilic C-2 position of phosphoenolpyruvate (PEP) leading to the cleavage of the C-O bond, whereas in most PEP-dependent enzymatic reactions PEP serves as a phosphoryl transfer agent (Figure 9). The only other known enolpyruvyl transfer from PEP to an OH group with the concomitant release of Pi occurs during the sixth step of the biosynthetic pathway of aromatic amino acids (the Shikimate pathway) in bacteria, plants and fungi, a reaction catalysed by 5-enolpyruvylshikimate-3-phosphate synthase AroA [50]. Even though MurA and AroA share 25% sequence identity and exhibit the

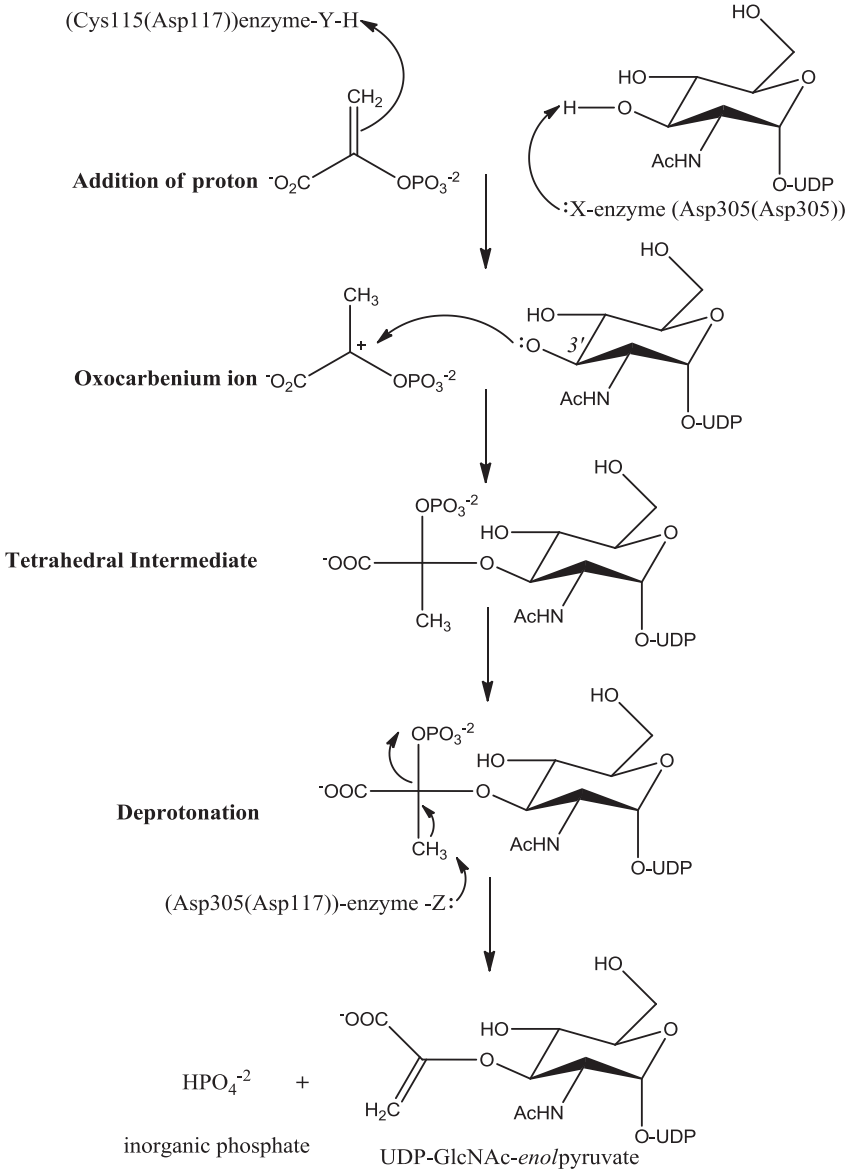

Figure 9. Mechanism of the addition–elimination reaction catalysed by MurA [52,53]. Catalytic residues of *M. tuberculosis* are shown in parenthesis.

same protein architecture, their reaction mechanisms appear to be substantially different [51].

The catalytic site is situated in a deep cavity between the two domains [53,54]. The reaction occurs through an induced-fit mechanism with large conformational changes in the two-domain structure of the enzyme. The active site loop of MurA shows a large deviation comprising 10 amino acids (Leu113-Arg122) connecting β2 with α2 in one of the subdomains. According to Schönbrunn et al. (1996) this loop is highly flexible [55]. In the mechanism of the addition–elimination reaction catalysed by MurA a proton is added to C-3 of PEP whereas the 3′-OH group of UDP-GlcNAc gets deprotonated. After formation of a tetrahedral intermediate, the elimination of phosphate results in the production of EP-UDP-GlcNAc (Figure 9) [50,53].

The natural product fosfomycin [(1*R*,2*S*)-1,2-epoxypropyl phosphonic acid], a broad-spectrum bactericidal antibiotic produced by *Streptomyces* sp., is known to selectively inhibit MurA. It is an epoxide that specifically inhibits MurA by forming a covalent adduct with a cysteine residue in the active site (Cys115 in both *E. coli* and *Enterobacter cloacae*; Cys117 in *Haemophilus influenzae*) [56]. However, fosfomycin has no activity against *M. tuberculosis*, since in the sequence of the *M. tuberculosis* MurA homologue, the key active site cysteine (amino acid 117 in the *M. tuberculosis* sequence) is replaced by an aspartic acid residue. A study revealed that the mutated enzyme is highly active but resistant to inactivation by fosfomycin [52].

The assay developed by Zhu and colleagues (2012) [49] revealed that the cysteine and aspartate side chains adopt similar positions and conformations in the PEP binding site through a general acid–base mechanism with rapid and reversible binding of PEP. The results of this study imply that the cysteine or aspartate residue at position 115 of *E. coli* (residue 117 in *M. tuberculosis*) performs the role of a general acid in the protonation of C-3 of PEP during the reaction. A candidate for the role of base in the initial deprotonation of the UDP-GlcNAc C-3 hydroxyl is Asp305 (in *M. tuberculosis* Asp305) [54]. In fact, Asp-305 must be responsible for the final proton abstraction from the C-3 atom of the PEP moiety required for the elimination of inorganic phosphate [57]. Other inhibitors of MurA based around a 2-aminotetralone motif [58] and other electrophilic natural products such as terreic acid [59] and cnicin [60] are covalent MurA inhibitors that essentially compete with PEP for reaction with Cys-115*via* a covalent mode of action involving the Cys115 thiol group of MurA.

The C115D enzyme (a mutant of MurA) lacks the ability to react with PEP covalently, a tight complex with UDPMurNAc cannot be formed, and the enzyme is presumably vulnerable to inhibition by a wider range of small molecule inhibitors that are able to interfere with the open-closed transition [50]. The alteration C117D in MurA of *M. tuberculosis* structure is confirmed as the key factor in innate resistance. Fosfomycin derivatives designed to bind in a MurA active site containing an aspartate rather than a cysteine residue may represent a route to production of novel drugs that are active against bacteria expressing an aspartyl-MurA [61].

2.7. MurB

UDP-N-acetylenolpyruvoylglucosamine reductase (MurB) catalyses the last step of the formation of UDP-N-acetylmuramic acid (UDPMurNAc). MurB catalyses the NADPH-dependent reduction of enolpyruvyl-UDP-N-acetylglucosamine (EP-UDP-NAc), yielding UDP-*N*-acetylmuramic acid (UDP-MurNAc) [62]. Subsequently, other enzymes in the pathway catalyse the sequential addition of three amino acids followed by a dipeptide. The gene *murB* is also essential in *E. coli* and *S. aureus*, as demonstrated by the isolation of temperature-sensitive mutants [63]. It is also important to point out that MurB is a flavoprotein that belongs to the FAD-binding protein superfamily and it shares a characteristic flavin adenine dinucleotide (FAD) binding fold [64]. These proteins contain one molecule of FAD as a cofactor and are proposed to transfer the protons from NADPH and solvent (water) to FAD and subsequently from $FADH_2$ to EP-UDPGlcNAc [62]. Considering that MurB is found in both gram positive and gram negative organisms it is expected that their inhibitors will possess broad spectrum antibacterial activity. As MurB has no known homologues in eukaryotes, it is a unique antibacterial target [62].

The overall reaction that is catalysed by MurB involves two half-reactions (Figure 10) in which the enzyme-bound FAD serves as the redox intermediate. The first half-reaction is the reduction of the FAD to $FADH_2$ by NADPH, which begins with the binding of NADPH to the enzyme and hydride transfer of the 4-*pro*-S hydrogen of NADPH to N-5 of an enzyme-bound flavin. The release of $NADP^+$ is followed by the binding of EP-UDPGlcNAc. The second half-reaction is the reduction of EP-UDPGlcNAc to UDPMurNAc in which hydride transfer occurs from the reduced flavin (Enz-$FADH_2$) to C-3 of the enolpyruvyl moiety of EP-UDP-GlcNAc. This is followed by formation a carbanion equivalent at C-2, which is stabilized by the α-carboxylate at C-1 as an enol intermediate. A solvent-equilibrated proton is then transferred to C-2, giving the UDPMurNAc product; this step returns the enzyme to the oxidized state [62]. The enzyme reaction catalysed by MurB is proceeds *via* a ping-pong mechanism, with weak and strong substrate inhibition by NADPH and EP-UDPGlcNAc, respectively [65].

MurB of *M. tuberculosis* contains 369 amino acid residues and is a mixed α + β protein comprised of three domains (Figure 11): In domain I (residues 21–86 and 364–369) the N- and C-terminals are located here, but domain I consists mainly of the N-terminal portion, Domain II (residues 90–244) and Domain III (residues 251–361). The domains I and II are involved in flavin binding while domain III is involved in substrate binding. The enzyme–substrate complex reveals three key residues (Arg159, Glu325 and Ser229 in *E. coli* and Arg176, Glu361 and Ser257 in *M. tuberculosis*) and a monovalent cation potentially involved in the catalytic process [67]. Both Glu-325 and Arg-159 are situated in close proximity to an oxygen of the enolpyruvylcarboxylate and are proposed to stabilize the enol intermediate by protonation. Ser229 is a catalytic residue and participates in the proton transfer to an enol intermediate that is formed during the second reduction step. The 3D modelled structure of MurB from *M. tuberculosis* is presented in Figure 11.

MurB is classified as Type I when it contains a Tyr loop (Tyr210 in *M. tuberculosis* and Tyr190 in *E. coli*) and split βαββ fold. MurB type II, lacks these secondary elements and contain a serine (Mtb) or a cysteine (*E. coli*) residue as a proton donor to quench the carbanionic intermediate [69]. A total of 11 highly conserved residues in several bacterial MurB proteins interact with the EP-UDP-GlcNAc or the cofactor FAD. Seven residues, including Asn71, Tyr175, Arg176, Arg213, Ser226, His259, and Glu296 (residues Asn71, Tyr175, Arg176, Arg238, Ser257, His324, and Glu361 in *M. tuberculosis*), were found to be essential for activity [68].

The first small-molecule inhibitors of MurB were tri-substituted thiazolidinones which were designed to mimic the diphosphate moiety of EP-UDP-GlcNAc and prepared by means of a parallel synthesis approach [70]. A series of imidazolinone analogues was synthesized and shown to possess potent MurB inhibitory as well as good antibacterial activity against *S. aureus* [71]. Over 195 4-alkyl and 4,4-dialkyl 1,2-bis(4-chlorophenyl)pyrazolidine-3,5-dione derivatives were synthesized for evaluation as new inhibitors of bacterial cell wall biosynthesis. Many of them demonstrated good activity against MurB *in vitro* and with low MIC values against gram-positive bacteria [72].

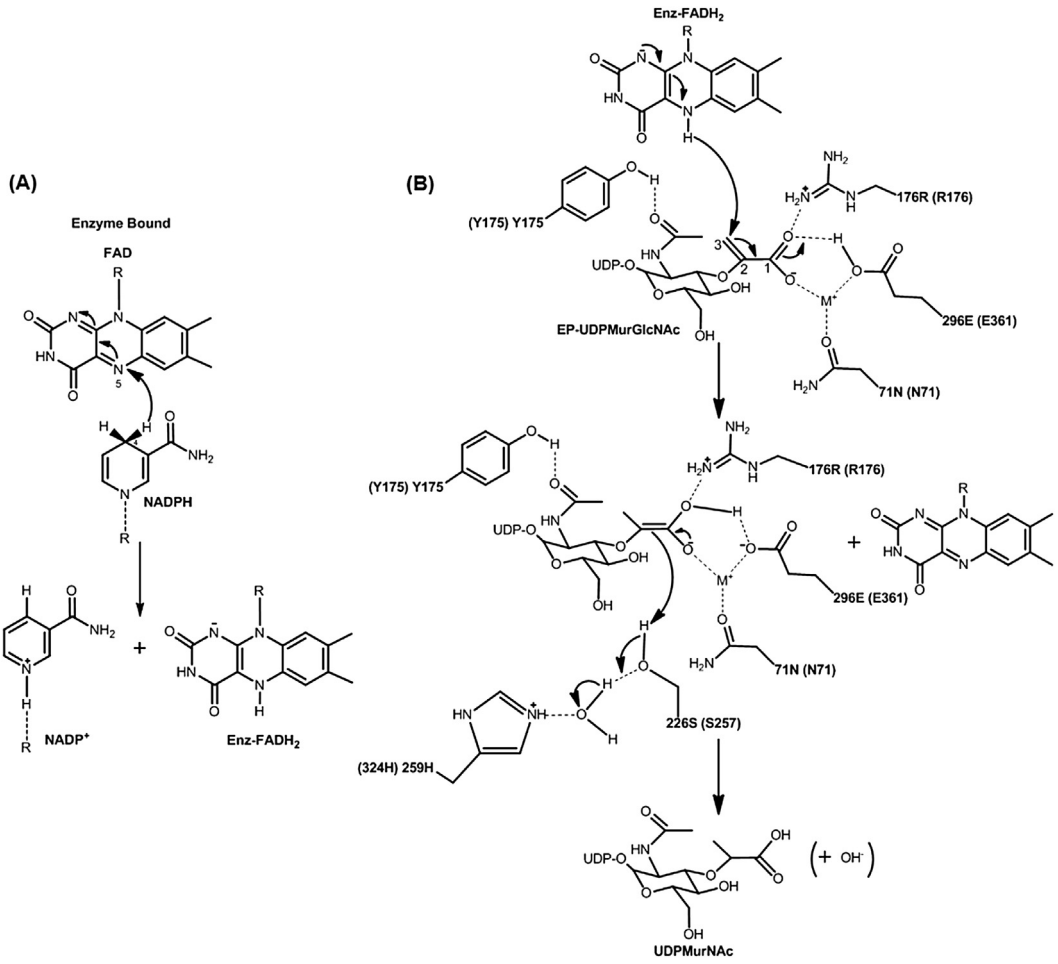

Figure 10. Reactions catalysed by MurB. Half-reaction for the transfer of the 4-pro-S hydride from NADPH to N-5 of Enz-FAD (A) [62] and transfer of hydride from Enz-$FADH_2$ to C-3 of the enolpyruvyl moiety of UDP-GlcNAc-enolpyruvate (B) [66]. M^+ indicates the location of the cationic ion. Catalytic residues of *M. tuberculosis* are shown in parenthesis.

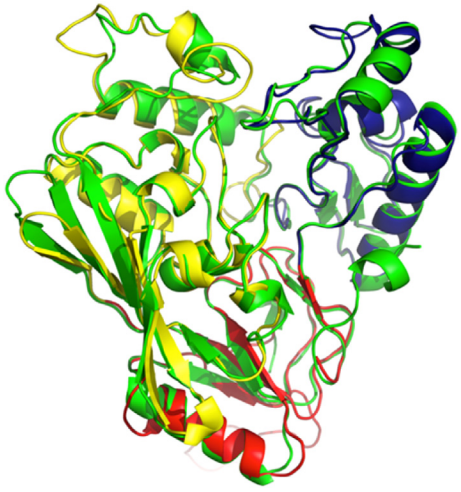

Figure 11. Superposition of the calculated MurB of *M. tuberculosis* (domain I, II and III is shown in red, yellow and blue, respectively) and *E. coli* (green lines – 1MBT) [68]. The 3D structure of the modelled enzyme is provided with the Supplementary material in PDB format. (For interpretation of the references to colour in this figure legend, the reader is referred to the web version of this article.)

In a study performed by Yang and colleagues (2006) [73] a set of 3,5-dioxopyrazolidines was identified as novel inhibitors of MurB. The resulting profile of the 3,5-dioxopyrazolidines reveals potent and specific inhibitors that bind within the active site of MurB adjacent to the FAD cofactor. These compounds display good activity against a range of gram-positive bacteria, including antibiotic-resistant strains. Many phenyl thiazolyl urea and carbamate derivatives also demonstrated good activity against MurA and MurB and gram-positive bacteria [74]. However, when these inhibitors were tested in the presence of bovine serum albumin (BSA),the activities for the pyrazolidine-3,5-dione series, phenyl thiazolyl urea and carbamate derivatives, were lost or declined [2].

2.8. Biosynthesis of the UDP-MurNAc-pentapeptides

The next cytoplasmic step in the biosynthesis of peptidoglycan involves a superfamily of four enzymes, the ATP-dependent amino acid ligases or the Mur ligases. After formation of UDP-MurNAc four enzymes sequentially catalyse the ligation and polymerization of the pentapeptide chain. These are: UDP-N-acetylmuramoyl:L-alanine ligase (MurC), UDP-N-acetylmuramoyl-L-alanine:D-glutamate ligase (MurD), UDP-N-acetylmuramoyl-L-alanine-D-glutamate:meso-diaminopimelate ligase (MurE) and UDP-N-acetylmuramoyl-L-alanine-D-glutamate-meso-diaminopimelate:D-alanyl-D-alanine ligase (MurF) [75]. These enzymes catalyse the

formation of an amide or peptide bond with concomitant cleavage of ATP into ADP and an inorganic phosphate.

All four ligases have a similar enzymatic mechanism in which the free carboxylate is activated by phosphoryl transfer from ATP to form an acyl phosphate intermediate and ADP [64]. This is followed by nucleophilic attack of the amino group of the condensing amino acid (dipeptide) to the carbonyl carbon of the acyl phosphate, leading to the formation of a high-energy tetrahedral intermediate, which breaks down into amide (or peptide) and inorganic phosphate (Figure 12).

Studies have shown that the ligases share three characteristics in common: (1) they have the same reaction mechanism, a divalent cation, Mg^{2+}or Mn^{2+} is essential for the reaction, (2) they have a series of six invariant Mur residues in addition to an ATP-binding consensus sequence and (3) they have the same three-dimensional structures in three domains [2]. Because these enzymes are essential for bacteria and do not occur in eukaryotes they are attractive antibacterial drug targets.

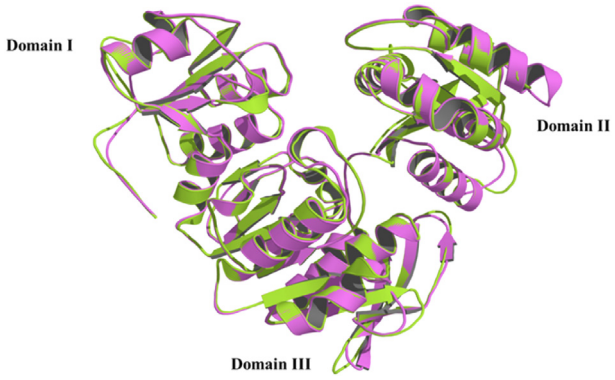

Figure 13. Superposition of the calculated MurC of *M. tuberculosis* (lemon) and *H. influenzae* (violet – PDB code: 1P31 [77]). The 3D structure of the modelled enzyme is provided with the Supplementary material in PDB format. (For interpretation of the references to colour in this figure legend, the reader is referred to the web version of this article.)

2.9. MurC

UDP-N-acetylmuramate-alanine ligase (MurC) is a non-ribosomal peptide ligase, which catalyses the addition of L-alanine to the nucleotide precursor UDP-N-acetylmuramoyl. This reaction requires ATP and produces ADP, inorganic phosphate and UDP-N-acetylmuramoyl-L-alanine (UMA) [77]. Interestingly, MurC of *M. tuberculosis* has *in vitro* specificity towards L-Ala; however, in an assay performed by Munshi and colleagues (2013) [78]. MurC of *M. tuberculosis* showed activity not only with L-Ala and Gly, but also with also with L-Ser. The comparative lower specificity for both L-Ser and Gly may be a possible reason for L-Ala being the preferred substrate [78]. The subsequent Mur synthetases are unable to use UDP-MurNAc-Gly or UDP-MurNAc-L-Ser or derivatives as substrates for propagating the reaction.

MurC has three α/β domains and consists of 494 amino acids composed of 17 helices (H1–H17) and 21 β-strands (1–21). Domain I or the UDP binding domain (residues 1–103) is located in N-terminal portion and consists of a central five-stranded, all-parallel β-sheet and four surrounding α-helices. This fold is reminiscent of the dinucleotide or Rossmann canonical G*x*G*xx*G binding, which is observed in many nucleotide-binding proteins. It contains a glycine-rich loop (Gly17, Gly19 and Gly20, in *M. tuberculosis*) between β1and H1 for the binding of the phosphate groups in UDP-Nacetylmuramoyl-L-alanine [77]. Domain II or the ATP binding (104–330), is the largest of the three domains of MurC, with a central seven-stranded, mostly parallel β-sheet surrounded by six helical segments and flanked by a small three-stranded, antiparallel β-sheet. Such folding is similar in many ATP-binding proteins [79] including all four of the Mur ligases. Domain III or the ligand binding part (residues 330–494) is located in the C-terminal portion and consists of a central six-stranded β-sheet with five parallel β-strands and one antiparallel, flanked by five α-helices. This domain contains a classic Rossmann dinucleotide-binding fold (Figure 13).

Biochemical kinetic results indicate that ATP is the first substrate to bind, UDP-MurNAc second and L-Ala third [80]. The MurC ATP-binding site lies at the interface between the second and third domains with key interactions with the adenine ring and α- and β-phosphates provided by residues in the ATP-binding domain [77]. The triphosphate is anchored by hydrogen bonds from the side chain of Lys126 (invariant in all Mur enzymes) [81]. Two residues that assist with the binding of an essential Mg^{2+} ion are Glu172 and Thr130 in *H. influenzae*, and the conserved residues Glu170 and Thr130 in *M. tuberculosis*. A second Mg^{2+} ion plays a role in stabilizing the interaction between the γ-phosphate and the free carboxylate during phosphoryl transfer. This second Mg^{2+} ion in *E. coli* is bound by the side chain of His199 (residue His195 in *M. tuberculosis*) and surrounded by water molecules, which are in turn stabilized by hydrogen bonding to several conserved residues, namely Asp198, His354 and Glu177 (residue Asp194, His354 and Glu173 in *M. tuberculosis*) [82]. According to Deva et al. (2006) the substrate binds in a cleft formed by the β2-α2 and β4-α4 loops, with the uracil ring sandwiched between hydrophobic residues from the two loops (Leu51 and Ile88 in *E. coli* and Ala42 and Ile84 in *M. tuberculosis*) and a hydrogen bond with the conserved His70 (His62 in *M. tuberculosis*) further holds the uracil ring in place. The ribose moiety interacts through both hydroxyl groups with the side chain of Asp49 and the diphosphate is hydrogen bonded to the side chain of Ser84 and the main-chain amide N atoms of a glycine-rich loop [82].

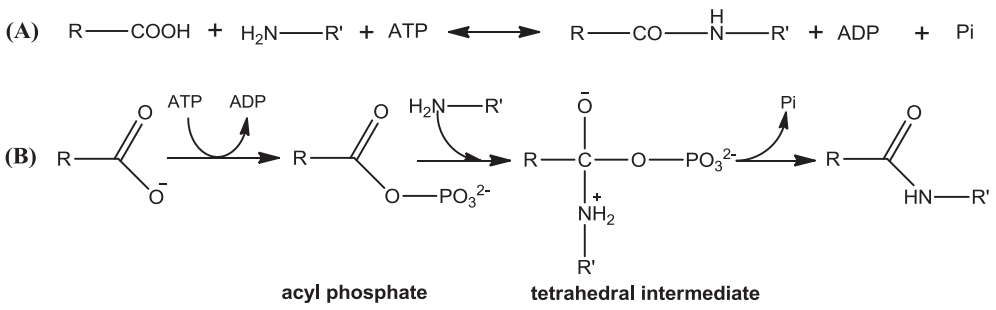

Figure 12. Reaction of the Mur ligases (A). Reaction mechanism of the Mur ligases (B) [76].

Biochemical studies show that MurC from *E. coli* exists in equilibrium between monomeric and dimeric forms, with a K_d of approximately 1 μM, and that it appears to have activity in both forms. The dimer interface is formed by the interaction of loops from the top of domain II of one molecule with loops from domain I of the second molecule and the most important interactions involve Phe223 and Tyr224 [83], however in *M. tuberculosis* the corresponding residues are not conserved (Pro218 and Gly219).

Site-directed mutagenesis of *E. coli* MurC identifies three residues as being critical for catalysis Lys130, Glu174, Asp351 (Lys126, Glu170 and Glu358, in *M. tuberculosis*) [84]. In a study by Kurokawa et al. (2008) [85] role of His343 in L-alanine recognition for *S. aureus* MurC was examined using both *in vitro* and *in vivo* assays. The results suggest that His343 is normally required for high-affinity binding of L-Ala to MurC at least at the restrictive temperature. They also provided experimental evidence supporting the structural information of MurC ligase [85]. In a systematic high throughput screening search for new antibacterial agents, benzylidene rhodanine (IC_{50} = 27 μM) was discovered as a promising inhibitor of MurC [86]. A series of phosphinate transition-state analogues were synthesized and tested on the *E. coli* MurC enzyme and a potent inhibitor with an IC_{50} of 49 μM was identified [87]. Analogues of L-alanine were tested as inhibitors for *E. coli* MurC and were shown to be competitive *versus* L-alanine but without specifying the type of inhibition [87–89].

2.10. MurD

UDP-N-acetylmuramoyl-L-alanine-D-glutamate ligase (MurD) is a cytoplasmic enzyme that catalyses addition of D-glutamate to the nucleotide precursor UDP-N-acetylmuramoyl-L-alanine (UMA) in the peptidoglycan biosynthetic pathway [90]. MurD is therefore an important target for inhibition of cell wall biosynthesis and consequently that of the growth of the organism [5]. It has a molecular weight of 49.3 kDa and is expressed in the cytoplasm as a single chain monomer with a length of 496 amino acids [91]. The enzymes from *E. coli*, [92] *S. aureus* [66], *H. influenzae* and *Enterococcus faecalis* [93] have been purified and characterized. MurD ligase from *E. coli* yielded the first reported crystal structure in which the enzyme was complexed with UDP MurNAc-L-Ala [94].

The catalytic mechanism of *E. coli* MurD for the catalysis of the peptide bond formation reaction between UDP-N-acetylmuramoyl-L-alanine (UMA) and D-glutamate (D-Glu) is well established [91,95]. Initially, MurD catalyses the ATP dependent phosphorylation of the UMA carboxylic acid. The resulting acyl-phosphate is then attacked by the incoming D-Glu to form a high-energy tetrahedral intermediate, which finally collapses into the amide product, UDP-*N*-acetylmuramoyl-L-alanine-D-glutamate (UMAG) and inorganic phosphate [91]. This mechanism is central to all the amide ligases families including the Mur ligases, which were confirmed by X-ray diffraction analysis [96], isotope transfer [97] and rapid quench [80] experiments. Studies have shown that *M. tuberculosis* MurD is enzymatically/structurally similar to *E. coli* MurD (PDB code: 1EEH, 1UAG and 2JFF) [98] with a protein sequence identity of 31% and similarity of 45% respectively [91]. Moreover, this enzyme in *M. tuberculosis* has been suggested as a broad-spectrum target for the design of antibacterial drugs [91,99] since it is essential for the survival of the organism [100]. However, the three dimensional structure of *M. tuberculosis* MurD is not yet known. A search was carried out against Protein Data Bank (PDB) using the *M. tuberculosis* MurD sequence, and a number of homologous sequences were retrieved. Among the sequences, the 2JFG crystal structure of *E. coli* MurD ligase [101] was selected as the best template (at 1.52 Å resolution) to build the *M. tuberculosis* MurD ligase homology model.

The amino acid sequences of MurD of *E. coli* (PDB code: 2JFG) [101] and *M. tuberculosis* share 32% identity and 45% sequence similarity. The MurD ligase has three domains *viz* (Figure 14). The N-terminal, central and the C-terminal domains respectively and all three domains belong to alpha and beta (α/β) class, in agreement with literature [91,101] The sequence alignment between the target ligase with a known crystal structure 2JFG [101] show the key residues which are involved in the substrate binding in *E. coli* MurD are Leu15, Thr16, Thr36, Arg37, Gly73, Asn138, Gln162 and His183 (corresponding residues in *M. tuberculosis* are Val18, Thr19, Asp39, Asp40, Gly75, Asn147, Gln171 and His192, respectively) [90,91,96]. Also, the residues for the ATP binding in *E. coli* are Gly114, Lys115, Ser116, Thr117, Glu157, Asn271, Arg302 and Asp317 (corresponding residues in *M. tuberculosis* are Gly123, Lys124, Thr125, Thr126, Glu166, Asp283 and Arg314, respectively) [91]. Finally, residues involved in the glutamic acid binding pocket are Lys348, Ser415 and Phe422 (corresponding residues in *M. tuberculosis* are Arg382, Ser463 and Tyr470, respectively) [91,101]. The 3D modelled structure of MurD from *M. tuberculosis* is presented in Figure 14.

2.11. MurE

UDP-N-acetylmuramoylalanyl-D-glutamate-2,6-diaminopimelate ligase (MurE) is the ATP-dependent ligase which incorporates amino acids including *meso*-diaminopimelic acid (*m*-DAP) into peptidoglycan during synthesis in a species-specific manner [3]. The third amino acid of the peptide system is generally either *meso*-A_2pm (most Gram-negative bacteria and bacilli) or L-lysine (most Gram-positive bacteria), although in certain species, other amino acids are encountered, for example, L-ornithine, LL-A_2pm, *meso*-lanthionine, L-diaminobutyric acid and L-homoserine [3,78]. Mengin and colleagues (1999) [102] have shown that the MurE enzyme is highly specific for the relevant amino acid, for example, when the third amino acid for *E. coli* is L-Lys, it leads to cell lysis. *Bacillus sphaericus* possesses two MurE enzymes: one with L-Lys in the third position which is active during vegetative growth, and one that adds *meso*-A_2pm that is active during spore cortex formation [103]. As for the second amino acid in the chain, certain variants of the third amino acid (amidated *meso*-A_2pm) necessitate a subsequent enzymatic activity [104]. In addition to that, *B. sphaericus* and *E. coli* are strongly activated by phosphate, a by-product of the reaction [103,105]. Research on *E. coli* MurE has shown that few analogues of *meso*-A_2pm (LL-A_2pm, lanthionine and cystathionine) are tolerated as substrates either *in vitro* orin genetically engineered cells [103–107].

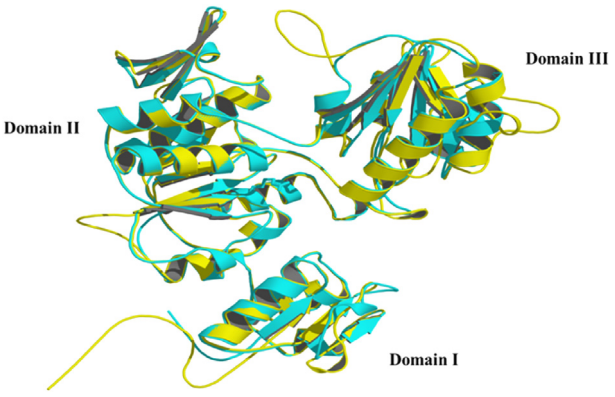

Figure 14. Superposition of the MurD protein of *M. tuberculosis* (yellow) and *E. coli* (blue – PDB code: 2JFG) [101]. The 3D structure of the modelled enzyme is provided with the Supplementary material in PDB format. (For interpretation of the references to colour in this figure legend, the reader is referred to the web version of this article.)

Comparison of the specificities of the MurE enzymes from a Gram negative (*E. coli*) and a Gram-positive (*S. aureus*) species towards the amino acid substrate was made. Whereas the *E. coli* enzyme has a very weak L-Lys-adding activity and the *S. aureus* MurE is totally unable to add *meso*-A_2pm [2,108]. Furthermore, *E. coli* MurE does not accept L-Orn as a substrate, contrary to the *staphylococcal* enzyme, which exhibits a weak L-Orn adding activity [2]. In at least two species, the MurE enzyme appears to be devoid of strict specificity. MurE from *Bifidobacterium globosum* incorporates two amino acids differently, namely L-Lys and L-Orn; both are retrieved in the peptidoglycan [109]. Peptidoglycan from MurE *Thermotoga maritima* is a Gram-negative species which contains similar proportions of both enantiomers of lysine, but no *meso*-A_2pm [110]. It adds L-Lys, D-Lys and *meso*-A_2pm *in vitro* with comparable efficiencies [111]. These authors have shown that the for UDP-MurNAc-tripeptide products the D-Glu-L-Lys bond has the conventional $\gamma \rightarrow \alpha$ arrangement; however, the ε-amino group of D-Lys is acylated, leading to the synthesis of a new nucleotide, UDP-MurNAc-L-Ala-D-Glu ($\gamma \rightarrow \varepsilon$) D-Lys [111]. The absence of *meso*-A_2pm in *T. maritima* peptide glycan is explained by the very low intracellular abundance of this compound [3,111].

Structural and functional characterization of *M. tuberculosis* MurE was reported [3]. This study involved the X-ray structure of MurE *M. tuberculosis* complexed toUAG (UDP-MurNAc-L-Ala-D-Glu) substrate and a magnesium ion (Figure 15). The asymmetric unit of the crystal contains 4 copies of the protein (chains A, B, C and D) (PDB code 2WTZ) [3]. Each copy has three domains consisting of residues 25–139, 140–378 and 379–535 and the UAG ligand binds to both domains I and II with the UDP portion binding to domain I and the peptide to domain II. Already, the third domain of copies A and B are more or less completely defined, but have a significantly higher B factor than domains I and II. For copies C and D there are considerable gaps in the third domain model as the domain is free to move significantly within the crystal [3]. The first 24 residues at the N-terminus are not visible in any chain. Chain A lacks residues 52–53 and there are extensive gaps in chains C and D due to the poor quality of the crystal structure. Chains A and B are incomplete and ends at 533. Chain C goes up to residues 505 and Chain D to residues 527. Several side chains were not modelled due to quality of the crystal structure [3]. In MurE *M. tuberculosis*, the first domain is the most divergent from the MurE *E. coli* structure (PDB code 1E8C) [112], it is actually closer to that of MurF *E. coli* (PDB code 1GG4) [3,113]. In particular the end chain of the β sheet in MurE *M. tuberculosis* and the MurF *E. coli* and *Streptococcus pneumoniae* structures is the N-terminal strand, but for the MurE *E. coli* sequence the end chain corresponds to β4, formed by a loop between β3 and β5 [3]. The 3D modelled structure of MurE from *M. tuberculosis* is presented in Figure 15.

Herein, we have decided modelling MurE with the same propose that we have modelled GlmU that was just to evaluate the homology modelling protocol used to build the other protein models. The crystal structure of MurE from *M. tuberculosis* (PDB code: 2XJA, 507 amino acid residues and 3.0 Å resolution) [3] was used as template to build MurE model (581 amino acid residues).

Basavannacharya and colleagues (2010) [3] have shown that MurE *M. tuberculosis* substrate complex superimpose well on all three domains of the *E. coli* MurE product complex, which is not as open as the MurF *E. coli* apo structure, but significantly more open than for the structure of MurF *Streptococcus pneumonia* complexed to inhibitors [3]. It is expected that during the peptide bond formation step, domain III will be more closely packed to domains I and II as is the case with the MurF *S. pneumonia* inhibitor structure. This indicates that the MurE *E. coli* product complex is in an open form on the way to product release, due to the fairly poor density seen for the diaminopimelate portion of the product, for which the B factor was double the value of the rest of the structure [112].

The substrate molecule UAG is bound between domains I and II in a very similar position to the product UMT (UDP-MurNAc-L-Ala-D-Glu-m-DAP) in the *E. coli* structure. Extensive hydrogen bonding interactions between UMT and the uracil ring of the UDP moiety of UAG is observed. These hydrogen bond interactions involve residues in the loop connecting β2 and β3 in domain I, and where the pyrophosphate moiety makes H-bonds with the main chain of the loop connecting β3 and β3 in domain I [3]. The O60 oxygen of the N-acetylmuramic acid ring forms a hydrogen bond with the Glu198 carboxylate in domain II, a conserved residue in the MurE family. O19 of the carbonyl group of the peptide bond of UAG interacts with NH1 and NH2 of Arg230 that is again also highly conserved. The α-carboxyl group of D-Glu forms a hydrogen bond with the alpha nitrogen of Thr195 and the side chain alcohol group of Ser222 [3].

Interestingly, residues Tyr194, Asp182, Lys115 and Lys196 in the active site of MurD *E. coli* are forming H-bond interactions with the substrate (corresponding residues in *M. tuberculosis* MurE are Tyr258, Asp247, Lys157 and Lys262, respectively) [3]. As described by Basavannacharya and co-workers, this modification of a lysine is found in many of the Mur ligases. The residues in the second coordination shell of the magnesium ion in MurD *E. coli* that are not conserved in *M. tuberculosis* MurE are Ser321, which can be substituted by the side chain of His395 in MurE, and Lys348 where Lys 396 NZ of MurE lies in an equivalent position. The second

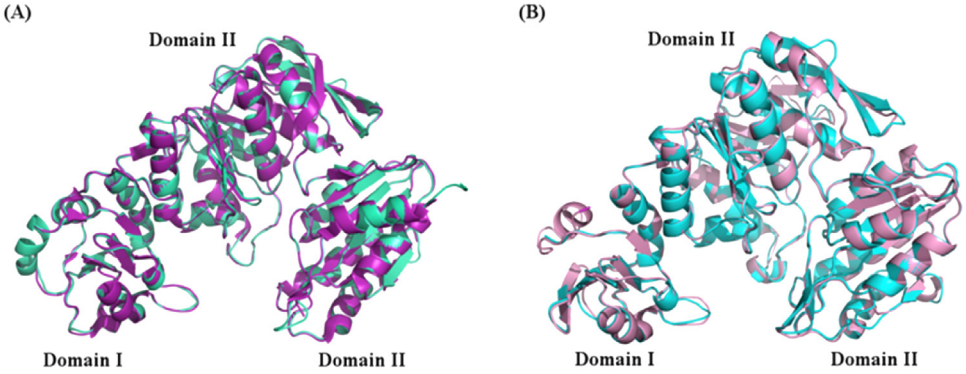

Figure 15. (A) Superposition of the calculated MurE of *M. tuberculosis* model building by homology (cyan) using template 2XJA [3,114] crystal structure (purple) from *M. tuberculosis*. (B) Superposition of the calculated MurE of *M. tuberculosis* model building by homology (cyan) using template 1E8C [112] crystal structure (pink) from *E. coli*. The 3D structure of the modelled enzyme is provided with the Supplementary material in PDB format. (For interpretation of the references to colour in this figure legend, the reader is referred to the web version of this article.)

magnesium ion seen in the *E. coli* MurD binding site is not found in the *M. tuberculosis* MurE structure as ADP is one of the direct ligands to that ion and there is no ADP/ATP present [3].

2.12. MurF

MurF (UDP-N-acetylmuramoylalanyl-D-glutamyl-2,6-diaminopimelate-D-alanyl-D-alanyl ligase) catalyses the addition of dipeptide D-Ala-D-Ala to the UDPMurNAc-tripeptide [3,113,115,116]. All four enzymes utilize ATP while incorporating peptides sequentially to the C-terminus of the peptide chain in a non-ribosomal fashion; they have been suggested to share a similar reaction mechanism [113]. As MurF has no human counterpart, it represents an attractive target for the development of new antibacterial drugs.

MurF *E. coli* was purified and studied, and as was the case with MurC, it follows a sequential, ordered kinetic mechanism [115,117]. Anderson and colleagues (1996) [115] studied two forms of UDP-MurNAc-tripeptide (meso-A_2pm and L-Lys) and they have shown that both are equally effective as substrates. They also demonstrated that and excess UDP-MurNAc-tripeptide leads to strong inhibition of this enzyme. The specificity profile for the dipeptide substrate has been the subject of many studies. Van Heijenoort, used *in vivo* systems with dipeptide substrate, showed that the results obtained are indirect [7]. However, when the pure enzyme is available, it has a high degree of specificity for the C-terminal amino acid [117,118]. Other research results have shown that this is complementary to the specificity of D-Ala (D-Alaligase or Ddl), which resides mainly on the N-terminal amino acid, and this constitutes a 'double sieving' mechanism that ensures the synthesis of UDP-MurNAc-pentapeptide ending mainly with D-Ala-D-Ala [120]. An interesting observation is the ability of MurF to incorporate the dipeptide 3-fluoro-D-Ala-3-fluoro-D-Ala, which is synthesized by Ddl *in vivo*, thereby explaining the auto antagonistic effect of high concentrations of the antibiotic 3-fluoro-D-Ala [117,119]. In addition, Boniface and colleagues (2006) [111] have studied the MurF enzyme from *T. maritima*. They have isolated the enzyme and demonstrated that it adds D-Ala-D-Ala to the L-Lys-containing UDP-MurNAc-tripeptide, but not to the D-Lys-containing nucleotide. However, the fact that the latter is a good substrate for MraY explains the incorporation of D-Lys into *T. maritima* peptidoglycan.

The crystallographic structure of MurF *E. coli* was determined (PDB code 1GG4) [113]. It contains three consecutive open α/β-sheet domains. The N-terminal domain is unique, while its central and C-terminal domains exhibit similar mononucleotide and dinucleotide-binding folds, respectively. The crystal structure of the apo-enzyme MurF *E. coli* reveals an open conformation with the three domains juxtaposed in a crescent-like arrangement creating a wide-open space where substrates are expected to bind. As such, catalysis is not feasible and significant domain closure is expected upon substrate binding [113]. Longenecker and colleagues (2005) [116] have obtained the crystallographic structure of the MurF *S. pneumonia* through NMR and X-ray crystallography. The NMR studies confirmed the specificity of binding to MurF and X-ray crystallography revealed the three-dimensional structure, yielding an observation that the protein–inhibitor complex adopts a dramatically different conformation than was found for the apo structure of MurF *E. coli* [113,116]. The 3D modelled structure of MurF from *M. tuberculosis* is presented in Figure 16.

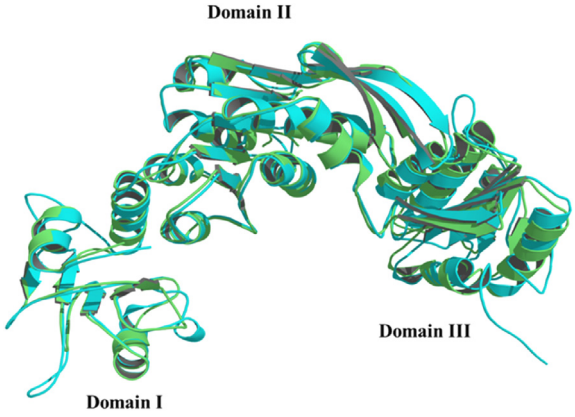

Figure 16. Superposition of the calculated MurF of *M. tuberculosis* (blue) and *S. pneumonia* (green – PDB code 2AM1 [116]). The 3D structure of the modelled enzyme is provided with the Supplementary material in PDB format. (For interpretation of the references to colour in this figure legend, the reader is referred to the web version of this article.)

The MurF ligase theoretical structure contains one asymmetric unit consisting of 510 residues that comprise three domains. The structures of the three domains individually are similar to those of the MurF homologue from *E. coli* (PDB code 1GG4) [113] and *S. pneumonia* (PDB code 2AM1) [116]. Moreover, the general descriptions of the fold for each of the three domains of the *E. coli* homologue suitably describe the corresponding structural elements for this newly determined structure [113,116]. The N-terminal domain (residues 1–81) is unique to MurF protein homologues, and consists of a small α/β fold. The central domain (residues 82–302) and the C-terminal domain (303–510) adopt mononucleotide and dinucleotide (Rossmann) folds, respectively, and are connected by a short linker peptide that is poorly ordered in the crystal of the template [116].

There is not much information about of the binding site from MurF *E. coli*. So, it is difficult to compare it with MurF *M. tuberculosis* in detail. In the report of the MurF *E. coli* structure, the investigators described an X-ray experiment in which they soaked a MurF crystal with two substrates, UDPMurNAc-tripeptide and D-Ala-D-Ala dipeptide and observed electron density for the uridine–ribose moiety located on the surface between the N-terminal and central domains. The uridine–ribose binding site unambiguously overlaps with the corresponding binding site [113]. Longenecker and co-workers (2005) [116] studied MurF *S. pneumonia* in complex with an inhibitor. The compounds studied were located at the interface between all three domains, laying on a hydrophobic shelf formed by Phe31 and Leu45 (residues Phe33 and Leu50 in *M. tuberculosis*) of the N-terminal domain and Tyr135 and Ile139 (residues Phe164 and Leu168 in *M. tuberculosis*)of the central domain. The most closely contacting residues were Asn326, Asn328, and Thr330 (residues Asn363, Asn365, and Asp367 in *M. tuberculosis*) of the C-terminal domain [116].

Finally, Table 1 shows a summary of validation results, sequence and templates used for building 3D structures of proteins studied. In general, the RMSD between targets and templates are close to 0.0 which shows that each target is spatially equivalent to its respective template. In addition, the stereochemical quality of each model was improved after refinement (Table 1). The QMEAN score of all structures are close to 1.0 which provides a good estimate of the absolute quality of the modelling structures in relating to reference structures solved by X-ray crystallography. Lastly, correct models should have LGscore >1.5 and the models reported here present LG scores higher than minimum expected (Table 1). More details about the modelled results are presented with the Supplementary material.

3. Conclusions

We believe that the present work provides useful information for the designing and synthesis of new inhibitors against TB, since

Table 1
Summary of the proteins studied here, where the values in parenthesis correspond to structures before of the refinement.

Protein	Sequence*	Ramachandran†	LG score	QMEAN score	Template	RMSD (Å)‡
GlmS	MT3542	90.6% (84.8%)	5.83 (1.03)	0.75 (0.06)	4AMV [21]	0.21
GlmM	MT3546	93.1% (91.8%)	6.23 (5.58)	0.87 (0.86)	3PDK [36]	0.81
GlmU	Rv1018c	94.7% (93.1%)	5.93 (6.02)	0.75 (0.72)	3D8V [40]	0.89
GlmU	Rv1018c	93.6% (91.2%)	5.53 (4.61)	0.70 (0.69)	1G97 [41]	0.63
MurA	MT1355	94.1% (93.2%)	5.09 (6.24)	0.79 (0.75)	3SWE [49]	0.25
MurB	MT0500	87.0% (89.0%)	5.74 (5.01)	0.73 (0.62)	1MBT [68]	0.48
MurC	MT2211	93.4% (92.4%)	4.55 (5.29)	0.79 (0.74)	3P31 [77]	0.26
MurD	MT2214	88.1% (86.9%)	3.86 (4.44)	0.66 (0.62)	2JFG [101]	0.37
MurE	MT2217	93.3% (93.1%)	5.91 (6.09)	0.85 (0.80)	2XJA [3,114]	0.27
MurE	MT2217	93.4% (91.2%)	5.89 (5.18)	0.78 (0.76)	1E8C [112]	0.30
MurF	MT2216	89% (88.7%)	4.11 (5.10)	0.69 (0.62)	1GG4 [113]	0.91

* http://www.tbdb.org/.
† Most favoured regions.
‡ RMSD calculated in PyMOL (The PyMOL Molecular Graphics System, Version 1.5.0.1 Schrödinger, LLC).

we have presented a detailed analysis about structure and function of the key enzymes from *M. tuberculosis* involved in peptidoglycan synthesis. In addition, the present study shows that molecular homology modelling is a useful tool to determine 3D structures of these proteins when their experimental 3D structures are not available.

Funding: UKZN, UPF and NRF (SA).

Competing interests: None declared.

Ethical approval: Not required.

Appendix A. Supplementary data

Supplementary data related to this article can be found at http://dx.doi.org/10.1016/j.tube.2015.01.006.

References

[1] World Health Organization. Global tuberculosis control: WHO report. 2013.
[2] Barreteau H, Kovač A, Boniface A, Sova M, Gobec S, Blanot D. Cytoplasmic steps of peptidoglycan biosynthesis. FEMS Microbiol Rev 2008;32:168–207. http://dx.doi.org/10.1111/j.1574-6976.2008.00104.x.
[3] Basavannacharya C, Robertson G, Munshi T, Keep NH, Bhakta S. ATP-dependent MurE ligase in Mycobacterium tuberculosis: biochemical and structural characterisation. Tuberculosis 2010;90:16–24. http://dx.doi.org/10.1016/j.tube.2009.10.007.
[4] Lamichhane G, Freundlich JS, Ekins S, Wickramaratne N, Nolan ST, Bishai WR. Essential metabolites of Mycobacterium tuberculosis and their mimics. mBio 2011;2:e00301–00310. http://dx.doi.org/10.1128/mBio.00301-10.
[5] Mahapatra S, Crick DC, Brennan PJ. Comparison of the UDP-N-acetylmuramate: L-alanine ligase enzymes from Mycobacterium tuberculosis and Mycobacterium leprae. J Bacteriol 2000;182:6827–30. http://dx.doi.org/10.1128/jb.182.23.6827-6830.2000.
[6] Mahapatra S, Basu J, Brennan PJ, Crick DC. Structure, biosynthesis and genetics of the mycolic acid-arabinogalactan-peptidoglycan complex. In: Cole ST, Eisenach KD, McMurray DN, Jacobs WR, editors. Tuberculosis and the Tubercle Bacillus. Washington, D.C.: ASM Press; 2005. p. 275–85.
[7] van Heijenoort J. Recent advances in the formation of the bacterial peptidoglycan monomer unit. Nat Product Rep 2001;18:503–19. http://dx.doi.org/10.1039/a804532a.
[8] Bouhss A, Trunkfield AE, Bugg TDH, Mengin-Lecreulx D. The biosynthesis of peptidoglycan lipid-linked intermediates. FEMS Microbiol Rev 2008;32:208–33. http://dx.doi.org/10.1111/j.1574-6976.2007.00089.x.
[9] Höltje HD, Sippl W, Rognan D, Folkers G. Molecular modeling: basic principles and applications. Weinheim: Wiley-VCH; 2008.
[10] Moraes G, Azevedo V, Costa M, Miyoshi A, Silva A, da Silva V, de Oliveira D, Teixeira MF, Lameira J, Alves CN. Homology modeling, molecular dynamics and QM/MM study of the regulatory protein PhoP from Corynebacterium pseudotuberculosis. J Mol Model 2012;18:1219–27. http://dx.doi.org/10.1007/s00894-011-1145-x.
[11] Lima AH, Souza PRM, Alencar N, Lameira J, Govender T, Kruger HG, Maguire GEM, Alves CN. Molecular modeling of T. rangeli, T. brucei gambiense, and T. evansi sialidases in complex with the DANA inhibitor. Chem Biol Drug Des 2012;80:114–20. http://dx.doi.org/10.1111/j.1747-0285.2012.01380.x.
[12] de Alencar NAN, Sousa PRM, Silva JRA, Lameira J, Alves CN, Marti S, Moliner V. Computational analysis of human OGA structure in complex with PUGNAc and NAG-thiazoline derivatives. J Chem Inform Model 2012;52:2775–83. http://dx.doi.org/10.1021/ci2006005.
[13] Honarparvar B, Govender T, Maguire GEM, Soliman MES, Kruger HG. Integrated approach to structure-based enzymatic drug design: molecular modeling, spectroscopy, and experimental bioactivity. Chem Rev 2014;114:493–537. http://dx.doi.org/10.1021/cr300314q.
[14] Durand P, Golinelli-Pimpaneau B, Mouilleron S, Badet B, Badet-Denisot M-A. Highlights of glucosamine-6P synthase catalysis. Arch Biochem Biophys 2008;474:302–17. http://dx.doi.org/10.1016/j.abb.2008.01.026.
[15] Milewski S, Gabriel L, Olchowy J. Enzymes of UDP-GlcNAc biosynthesis in yeast. Yeast 2006;23:1–14. http://dx.doi.org/10.1002/yea.1337.
[16] Wells L, Vosseller K, Hart GW. A role for N-acetylglucosamine as a nutrient sensor and mediator of insulin resistance. Cell Mol Life Sci 2003;60:222–8. http://dx.doi.org/10.1007/s000180300017.
[17] Traxinger RR, Marshall S. Coordinated regulation of glutamine-fructose-6-phosphate amidotransferase activity by insulin, glucose, and glutamine – role of hexosamine biosynthesis in enzyme regulation. J Biol Chem 1991;266:10148–54.
[18] Milewski S. Glucosamine-6-phosphate synthase-the multi-facets enzyme. Biochim Biophys Acta-Protein Struct Mol Enzym 2002;1597:173–92. http://dx.doi.org/10.1016/s0167-4838(02)00318-7.
[19] Teplyakov A, Leriche C, Obmolova G, Badet B, Badet-Denisot MA. From Lobry de Bruyn to enzyme-catalyzed ammonia channelling: molecular studies of D-glucosamine-6P synthase. Nat Product Rep 2002;19:60–9. http://dx.doi.org/10.1039/b103713g.
[20] Leriche C, BadetDenisot MA, Badet B. Characterization of a phosphoglucose isomerase-like activity associated with the carboxy-terminal domain of Escherichia coli glucosamine-6-phosphate synthase. J Am Chem Soc 1996;118:1797–8. http://dx.doi.org/10.1021/ja953614q.
[21] Mouilleron S, Badet-Denisot MA, Golinelli-Pimpaneau B. Glutamine binding opens the ammonia channel and activates glucosamine-6P synthase. J Biol Chem 2006;281:4404–12. http://dx.doi.org/10.1074/jbc.M511689200.
[22] Kenig M, Vandamme E, Abraham EP. Mode of action of bacilysin and anticapsin and biochemical properties of bacilysin-resistant mutants. J General Microbiol 1976;94:46–54.
[23] Mouilleron S, Badet-Denisot M-A, Badet B, Golinelli-Pimpaneau B. Dynamics of glucosamine-6-phosphate synthase catalysis. Arch Biochem Biophys 2011;505:1–12. http://dx.doi.org/10.1016/j.abb.2010.08.008.
[24] Teplyakov A, Obmolova G, Badet-Denisot MA, Badet B, Polikarpov I. Involvement of the C terminus in intramolecular nitrogen channeling in glucosamine 6-phosphate synthase: evidence from a 1.6 angstrom crystal structure of the isomerase domain. Struct Fold Des 1998;6:1047–55. http://dx.doi.org/10.1016/s0969-2126(98)00105-1.
[25] Winterbu PJ, Phelps CF. Binding of substrates and modifiers to glucosamine synthetase. Biochem J 1971;121:721.
[26] Floquet N, Richez C, Durand P, Maigret B, Badet B, Badet-Denisot M-A. Discovering new inhibitors of bacterial glucosamine-6P synthase (GlmS) by docking simulations. Bioorg Med Chem Lett 2007;17:1966–70. http://dx.doi.org/10.1016/j.bmcl.2007.01.052.
[27] Krahn JM, Kim JH, Burns MR, Parry RJ, Zalkin H, Smith JL. Coupled formation of an amidotransferase interdomain ammonia channel and a phosphoribosyltransferase active site. Biochemistry 1997;36:11061–8. http://dx.doi.org/10.1021/bi9714114.
[28] Isupov MN, Obmolova G, Butterworth S, BadetDenisot MA, Badet B, Polikarpov I, Littlechild JA, Teplyakov A. Substrate binding is required for assembly of the active conformation of the catalytic site in Ntn amidotransferases: evidence from the 1.8 angstrom crystal structure of the

glutaminase domain of glucosamine 6-phosphate synthase. Structure 1996;4:801–10. http://dx.doi.org/10.1016/s0969-2126(96)00087-1.
[29] Teplyakov A, Obmolova G, Badet-Denisot MA, Badet B. The mechanism of sugar phosphate isomerization by glucosamine 6-phosphate synthase. Protein Sci 1999;8:596–602.
[30] DeReuse H, Labigne A, MenginLecreulx D. The Helicobacter pylori ureC gene codes for a phosphoglucosamine mutase. J Bacteriol 1997;179:3488–93.
[31] Jolly L, Wu SW, vanHeijenoort J, deLencastre H, MenginLecreulx D, Tomasz A. The femR315 gene from Staphylococcus aureus, the interruption of which results in reduced methicillin resistance, encodes a phosphoglucosamine mutase. J Bacteriol 1997;179:5321–5.
[32] Glanzmann P, Gustafson J, Komatsuzawa H, Ohta K, Berger-Bachi B. glmM operon and methicillin-resistant glmM suppressor mutants in Staphylococcus aureus. Antimicrob Agents Chemother 1999;43:240–5.
[33] Tavares IM, Jolly L, Pompeo F, Leitao JH, Fialho AM, Sa-Correia I, Mengin-Lecreulx D. Identification of the Pseudomonas aeruginosa glmM gene, encoding phosphoglucosamine mutase. J Bacteriol 2000;182:4453–7. http://dx.doi.org/10.1128/jb.182.16.4453-4457.2000.
[34] Shimazu K, Takahashi Y, Uchikawa Y, Shimazu Y, Yajima A, Takashima E, Aoba T, Konishi K. Identification of the Streptococcus gordonii glmM gene encoding phosphoglucosamine mutase and its role in bacterial cell morphology, biofilm formation, and sensitivity to antibiotics. FEMS Immunol Med Microbiol 2008;53:166–77. http://dx.doi.org/10.1111/j.1574-695X.2008.00410.x.
[35] Mehra-Chaudhary R, Mick J, Tanner JJ, Beamer LJ. Quaternary structure, conformational variability and global motions of phosphoglucosamine mutase. FEBS J 2011;278:3298–307. http://dx.doi.org/10.1111/j.1742-4658.2011.08246.x.
[36] Mehra-Chaudhary R, Mick J, Beamer LJ. Crystal structure of Bacillus anthracis phosphoglucosamine mutase, an enzyme in the peptidoglycan biosynthetic pathway. J Bacteriol 2011;193:4081–7. http://dx.doi.org/10.1128/jb.00418-11.
[37] Mehra-Chaudhary R, Mick J, Tanner JJ, Henzl MT, Beamer LJ. Crystal structure of a bacterial phosphoglucomutase, an enzyme involved in the virulence of multiple human pathogens. Proteins-Struct Funct Bioinforma 2011;79:1215–29. http://dx.doi.org/10.1002/prot.22957.
[38] Jolly L, Ferrari P, Blanot D, van Heijenoort J, Fassy F, Mengin-Lecreulx D. Reaction mechanism of phosphoglucosamine mutase from Escherichia coli. Eur J Biochem 1999;262:202–10. http://dx.doi.org/10.1046/j.1432-1327.1999.00373.x.
[39] Mengin-Lecreulx D, Vanheijenoort J. Identification of the glmu gene encoding N-acetylglucosamine-1-phosphate uridyltransferase in Escherichia-coli. J Bacteriol 1993;175:6150–7.
[40] Zhang Z, Bulloch EMM, Bunker RD, Baker EN, Squire CJ. Structure and function of GlmU from Mycobacterium tuberculosis. Acta Crystallogr Sect D-Biol Crystallogr 2009;65:275–83. http://dx.doi.org/10.1107/s0907444909001036.
[41] Kostrewa D, D'Arcy A, Takacs B, Kamber N. Crystal structures of Streptococcus pneumoniae N-acetylglucosamine-1-phosphate uridyltransferase, GlmU, in apo form at 2.33 A resolution and in complex with UDP-N-acetylglucosamine and Mg2+ at 1.96 A resolution. J Mol Biol 2001;305:279–89. http://dx.doi.org/10.1006/jmbi.2000.4296.
[42] Parikh A, Verma SK, Khan S, Prakash B, Nandicoori VK. PknB-mediated phosphorylation of a novel substrate, N-acetylglucosamine-1-phosphate uridyltransferase, modulates its acetyltransferase activity. J Mol Biol 2009;386:451–64. http://dx.doi.org/10.1016/j.jmb.2008.12.031.
[43] Zhou Y, Yu W, Zheng Q, Xin Y, Ma Y. Identification of amino acids involved in catalytic process of M-tuberculosis GlmU acetyltransferase. Glycoconj J 2012;29:297–303. http://dx.doi.org/10.1007/s10719-012-9402-5.
[44] Maruyama D, Nishitani Y, Nonaka T, Kita A, Fukami TA, Mio T, Yamada-Okabe H, Yamada-Okabe T, Miki K. Crystal structure of uridine-diphospho-N-acetylglucosamine pyrophosphorylase from Candida albicans and catalytic reaction mechanism. J Biol Chem 2007;282:17221–30. http://dx.doi.org/10.1074/jbc.M611873200.
[45] Pereira MP, Blanchard JE, Murphy C, Roderick SL, Brown ED. High-throughput screening identifies novel inhibitors of the acetyltransferase activity of Escherichia coli GlmU. Antimicrob Agents Chemother 2009;53:2306–11. http://dx.doi.org/10.1128/aac.01572-08.
[46] Mochalkin I, Lightle S, Narasimhan L, Bornemeier D, Melnick M, Vanderroest S, McDowell L. Structure of a small-molecule inhibitor complexed with GlmU from Haemophilus influenzae reveals an allosteric binding site. Protein Sci 2008;17:577–82. http://dx.doi.org/10.1110/ps.073271408.
[47] Pompeo F, van Heijenoort J, Mengin-Lecreulx D. Probing the role of cysteine residues in glucosamine-1-phosphate acetyltransferase activity of the bifunctional GlmU protein from Escherichia coli: site-directed mutagenesis and characterization of the mutant enzymes. J Bacteriol 1998;180:4799–803.
[48] Burton E, Gawande PV, Yakandawala N, LoVetri K, Zhanel GG, Romeo T, Friesen AD, Madhyastha S. Antibiofilm activity of GlmU enzyme inhibitors against catheter-associated uropathogens. Antimicrob Agents Chemother 2006;50:1835–40. http://dx.doi.org/10.1128/aac.50.5.1835-1840.2006.
[49] Zhu J-Y, Yang Y, Han H, Betzi S, Olesen SH, Marsilio F, Schoenbrunn E. Functional consequence of covalent reaction of phosphoenolpyruvate with UDP-N-acetylglucosamine 1-carboxyvinyltransferase (MurA). J Biol Chem 2012;287:12657–67. http://dx.doi.org/10.1074/jbc.M112.342725.
[50] Walsh CT, Benson TE, Kim DH, Lees WJ. The versatility of phosphoenolpyruvate and its vinyl ether products in biosynthesis. Chem Biol 1996;3:83–91. http://dx.doi.org/10.1016/s1074-5521(96)90282-3.
[51] Byczynski B, Mizyed S, Berti PJ. Nonenzymatic breakdown of the tetrahedral (alpha-carboxyketal phosphate) intermediates of MurA and AroA, two carboxyvinyl transferases. Protonation of different functional groups controls the rate and fate of breakdown. J Am Chem Soc 2003;125:12541–50. http://dx.doi.org/10.1021/ja0349655.
[52] Kim DH, Lees WJ, Kempsell KE, Lane WS, Duncan K, Walsh CT. Characterization of a Cys115 to Asp substitution in the Escherichia coli cell wall biosynthetic enzyme UDP-GlcNAc enolpyruvyl transferase (MurA) that confers resistance to inactivation by the antibiotic fosfomycin. Biochemistry 1996;35:4923–8. http://dx.doi.org/10.1021/bi952937w.
[53] Skarzynski T, Kim DH, Lees WJ, Walsh CT, Duncan K. Stereochemical course of enzymatic enolpyruvyl transfer and catalytic conformation of the active site revealed by the crystal structure of the fluorinated analogue of the reaction tetrahedral intermediate bound to the active site of the C115A mutant of MurA. Biochemistry 1998;37:2572–7. http://dx.doi.org/10.1021/bi9722608.
[54] Skarzynski T, Mistry A, Wonacott A, Hutchinson SE, Kelly VA, Duncan K. Structure of UDP-N-acetylglucosamine enolpyruvyl transferase, an enzyme essential for the synthesis of bacterial peptidoglycan, complexed with substrate UDP-N-acetylglucosamine and the drug fosfomycin. Structure 1996;4:1465–74. http://dx.doi.org/10.1016/s0969-2126(96)00153-0.
[55] Schonbrunn E, Sack S, Eschenburg S, Perrakis A, Krekel F, Amrhein N, Mandelkow E. Crystal structure of UDP-N-acetylglucosamine enolpyruvyltransferase, the target of the antibiotic fosfomycin. Structure 1996;4:1065–75. http://dx.doi.org/10.1016/s0969-2126(96)00113-x.
[56] Kahan FM, Kahan JS, Cassidy PJ, Kropp H. Mechanism of action of fosfomycin (phosphonomycin). Ann N Y Acad Sci 1974;235:364–86. http://dx.doi.org/10.1111/j.1749-6632.1974.tb43277.x.
[57] Eschenburg S, Kabsch W, Healy ML, Schonbrunn E. A new view of the mechanisms of UDP-N-acetylglucosamine enolpyruvyl transferase (MurA) and 5-enolpyruvylshikimate-3-phosphate synthase (AroA) derived from X-ray structures of their tetrahedral reaction intermediate states. J Biol Chem 2003;278:49215–22. http://dx.doi.org/10.1074/jbc.M309741200.
[58] Dunsmore CJ, Miller K, Blake KL, Patching SG, Henderson PJF, Garnett JA, Stubbings WJ, Phillips SEV, Palestrant DJ, Angeles JDL, Leeds JA, Chopra I, Fishwick CWG. 2-Aminotetralones: novel inhibitors of MurA and MurZ. Bioorg Med Chem Lett 2008;18:1730–4. http://dx.doi.org/10.1016/j.bmcl.2008.01.089.
[59] Han H, Yang Y, Olesen SH, Becker A, Betzi S, Schonbrunn E. The fungal product terreic acid is a covalent inhibitor of the bacterial cell wall biosynthetic enzyme UDP-N-acetylglucosamine 1-carboxyvinyltransferase (MurA). Biochemistry 2010;49:4276–82. http://dx.doi.org/10.1021/bi100365b.
[60] Steinbach A, Scheidig AJ, Klein CD. The unusual binding mode of cnicin to the antibacterial target enzyme MurA revealed by X-ray crystallography. J Med Chem 2008;51:5143–7. http://dx.doi.org/10.1021/jm800609p.
[61] De Smet KAL, Kempsell KE, Gallagher A, Duncan K, Young DB. Alteration of a single amino acid residue reverses fosfomycin resistance of recombinant MurA from Mycobacterium tuberculosis. Microbiology-Uk 1999;145:3177–84.
[62] Benson TE, Marquardt JL, Marquardt AC, Etzkorn FA, Walsh CT. Overexpression, purification, and mechanistic study of Udp-N-acetylenolpyruvylglucosamine reductase. Biochemistry 1993;32:2024–30. http://dx.doi.org/10.1021/bi00059a019.
[63] Matsuo M, Kurokawa K, Nishida S, Lu Y, Takimura H, Kaito C, Fukuhara N, Maki H, Miura K, Murakami K, Sekimizu K. Isolation and mutation site determination of the temperature-sensitive murB mutants of Staphylococcus aureus. FEMS Microbiol Lett 2003;222:107–13. http://dx.doi.org/10.1016/s0378-1097(03)00260-x.
[64] Murzin AG. Structural classification of proteins: new superfamilies. Curr Opin Struct Biol 1996;6:386–94. http://dx.doi.org/10.1016/s0959-440x(96)80059-5.
[65] Dhalla AM, Yanchunas J, Ho HT, Falk PJ, Villafranca JJ, Robertson JG. Steady-state kinetic mechanism of Escherichia-coli Udp-N-acetylenolpyruvylglucosamine reductase. Biochemistry 1995;34:5390–402. http://dx.doi.org/10.1021/bi00016a010.
[66] Nishida S, Kurokawa K, Matsuo M, Sakamoto K, Ueno K, Kita K, Sekimizu K. Identification and characterization of amino acid residues essential for the active site of UDP-N-acetylenolpyruvylglucosamine reductase (MurB) from Staphylococcus aureus. J Biol Chem 2006;281:1714–24.
[67] Benson TE, Filman DJ, Walsh CT, Hogle JM. An enzyme-substrate complex involved in bacterial-cell wall biosynthesis. Nat Struct Biol 1995;2:644–53. http://dx.doi.org/10.1038/nsb0895-644.
[68] Benson TE, Walsh CT, Hogle JM. The structure of the substrate-free form of MurB, an essential enzyme for the synthesis of bacterial cell walls. Structure 1996;4:47–54. http://dx.doi.org/10.1016/s0969-2126(96)00008-1.
[69] Kim M-K, Cho MK, Song H-E, Kim D, Park B-H, Lee JH, Kang GB, Kim SH, Im YJ, Lee D-S, Eom SH. Crystal structure of UDP-N-acetylenolpyruvylglucosamine reductase (MurB) from Thermus caldophilus. Proteins-Struct Funct Bioinforma 2007;66:751–4. http://dx.doi.org/10.1002/prot.21174.

[70] Andres CJ, Bronson JJ, D'Andrea SV, Deshpande MS, Falk PJ, Grant-Young KA, Harte WE, Ho HT, Misco PF, Robertson JG, Stock D, Sun YX, Walsh AW. 4-Thiazolidinones: novel inhibitors of the bacterial enzyme MurB. Bioorg Med Chem Lett 2000;10:715–7. http://dx.doi.org/10.1016/s0960-894x(00)00073-1.

[71] Bronson JJ, DenBleyker KL, Falk PJ, Mate RA, Ho HT, Pucci MJ, Snyder LB. Discovery of the first antibacterial small molecule inhibitors of MurB. Bioorg Med Chem Lett 2003;13:873–5. http://dx.doi.org/10.1016/s0960-894x(02)01076-4.

[72] Kutterer KMK, Davis JM, Singh G, Yang YJ, Hu W, Severin A, Rasmussen BA, Krishnamurthy G, Failli A, Katz AH. 4-Alkyl and 4,4′-dialkyl 1,2-bis(4-chlorophenyl)pyrazolidine-3,5-dione derivatives as new inhibitors of bacterial cell wall biosynthesis. Bioorg Med Chem Lett 2005;15:2527–31. http://dx.doi.org/10.1016/j.bmcl.2005.03.058.

[73] Yang YJ, Severin A, Chopra R, Krishnamurthy G, Singh G, Hu W, Keeney D, Svenson K, Petersen PJ, Labthavikul P, Shlaes DM, Rasmussen BA, Failli AA, Shumsky JS, Kutterer KMK, Gilbert A, Mansour TS. 3,5-Dioxopyrazolidines, novel inhibitors of UDP-N-acetylenolpyruvylglucosamine reductase (MurB) with activity against gram-positive bacteria. Antimicrob Agents Chemother 2006;50:556–64. http://dx.doi.org/10.1128/aac.50.2.556-564.2006.

[74] Francisco GD, Li Z, Albright JD, Eudy NH, Katz AH, Petersen PJ, Labthavikul P, Singh G, Yang YJ, Rasmussen BA, Lin YI, Mansour TS. Phenyl thiazolyl urea and carbamate derivatives as new inhibitors of bacterial cell-wall biosynthesis. Bioorg Med Chem Lett 2004;14:235–8. http://dx.doi.org/10.1016/j.bmcl.2003.09.082.

[75] Smith CA. Structure, function and dynamics in the mur family of bacterial cell wall ligases. J Mol Biol 2006;362:640–55. http://dx.doi.org/10.1016/j.jmb.2006.07.066.

[76] Bouhss A, Dementin S, van Heijenoort J, Parquet C, Blanot D. Formation of adenosine 5′-tetraphosphate from the acyl phosphate intermediate: a difference between the MurC and MurD synthetases of Escherichia coli. Febs Lett 1999;453:15–9. http://dx.doi.org/10.1016/s0014-5793(99)00684-5.

[77] Mol CD, Brooun A, Dougan DR, Hilgers MT, Tari LW, Wijnands RA, Knuth MW, McRee DE, Swanson RV. Crystal structures of active fully assembled substrate- and product-bound complexes of UDP-N-acetylmuramic acid: L-alanine ligase (MurC) from Haemophilus influenzae. J Bacteriol 2003;185:4152–62. http://dx.doi.org/10.1128/jb.185.14.4152-4162.2003.

[78] Munshi T, Gupta A, Evangelopoulos D, Guzman JD, Gibbons S, Keep NH, Bhakta S. Characterisation of ATP-dependent Mur ligases involved in the biogenesis of cell wall peptidoglycan in Mycobacterium tuberculosis. Plos One 2013:8. http://dx.doi.org/10.1371/journal.pone.0060143.

[79] Denessiouk KA, Johnson MS. When fold is not important: a common structural framework for adenine and AMP binding in 12 unrelated protein families. Proteins-Struct Funct Genet 2000;38:310–26. 10.1002/(sici)1097-0134(20000215)38:3<310::aid-prot7>3.0.co;2-t.

[80] Emanuele JJ, Jin HY, Yanchunas J, Villafranca JJ. Evaluation of the kinetic mechanism of Escherichia coli uridine diphosphate-N-acetylmuramate:L-alanine ligase. Biochemistry 1997;36:7264–71. http://dx.doi.org/10.1021/bi970266r.

[81] Spraggon G, Schwarzenbacher R, Kreusch A, Lee CC, Abdubek P, Ambing E, Biorac T, Brinen LS, Canaves JM, Cambell J, Chin HJ, Dai XP, Deacon AM, DiDonato M, Elsliger MA, Eshagi S, Floyd R, Godzik A, Grittini C, Grzechnik SK, Hampton E, Jaroszewski L, Karlak C, Klock HE, Koesema E, Kovarik JS, Kuhn P, Levin I, McMullan D, McPhillips TM, Miller MD, Morse A, Moy K, Ouyang J, Page R, Quijano K, Robb A, Stevens RC, van den Bedem H, Velasquez J, Vincent J, von Delft F, Wang XH, West B, Wolf G, Xu QP, Hodgson KO, Wooley J, Lesley SA, Wilson IA. Crystal structure of an Udp-n-acetylmuramate-alanine ligase MurC (TM0231) from Thermotoga maritima at 2.3 angstrom resolution. Proteins-Struct Funct Bioinforma 2004;55:1078–81. http://dx.doi.org/10.1002/prot.20034.

[82] Deva T, Baker EN, Squire CJ, Smith CA. Structure of Escherichia coli UDP-N-acetylmuramoyl: L-alanine ligase (MurC). Acta Crystallogr Sect D-Biol Crystallogr 2006;62:1466–74. http://dx.doi.org/10.1107/s0907444906038376.

[83] Jin HY, Emanuele JJ, Fairman R, Robertson JG, Hail ME, Ho HT, Falk PJ, Villafranca JJ. Structural studies of Escherichia coli UDP-N-acetylmuramate: L-alanine ligase. Biochemistry 1996;35:1423–31. http://dx.doi.org/10.1021/bi952334k.

[84] Bouhss A, MenginLecreulx D, Blanot D, vanHeijenoort J, Parquet C. Invariant amino acids in the mur peptide synthetases of bacterial peptidoglycan synthesis and their modification by site-directed mutagenesis in the UDP-MurNAc:L-alanine ligase from Escherichia coli. Biochemistry 1997;36:11556–63. http://dx.doi.org/10.1021/bi970797f.

[85] Kurokawa K, Nishida S, Ishibashi M, Mizumura H, Ueno K, Yutsudo T, Maki H, Murakami K, Sekimizu K. Staphylococcus aureus MurC participates in L-alanine recognition via histidine 343, a conserved motif in the shallow hydrophobic pocket. J Biochem 2008;143:417–24. http://dx.doi.org/10.1093/jb/mvm237.

[86] Sim MM, Ng SB, Buss AD, Crasta SC, Goh KL, Lee SK. Benzylidene rhodanines as novel inhibitors of UDP-N-acetylmuramate/L-alanine ligase. Bioorg Med Chem Lett 2002;12:697–9. http://dx.doi.org/10.1016/s0960-894x(01)00832-0.

[87] Reck F, Marmor S, Fisher S, Wuonola MA. Inhibitors of the bacterial cell wall biosynthesis enzyme MurC. Bioorg Med Chem Lett 2001;11:1451–4. http://dx.doi.org/10.1016/s0960-894x(01)00251-7.

[88] Liger D, Masson A, Blanot D, Vanheijenoort J, Parquet C. Over-production, purification and properties of the uridine-diphosphate-N-acetylmuramate-L-alanine ligase from Escherichia-coli. Eur J Biochem 1995;230:80–7. http://dx.doi.org/10.1111/j.1432-1033.1995.0080i.x.

[89] Emanuele JJ, Jin HY, Jacobson BL, Chang CYY, Einspahr HM, Villafranca JJ. Kinetic and crystallographic studies of Escherichia coli UDP-N-acetylmuramate:L-alanine ligase. Protein Sci 1996;5:2566–74.

[90] Bertrand JA, Fanchon E, Martin L, Chantalat L, Auger G, Blanot D, van Heijenoort J, Dideberg O. "Open" structures of MurD: domain movements and structural similarities with folylpolyglutamate synthetase. J Mol Biol 2000;301:1257–66. http://dx.doi.org/10.1006/jmbi.2000.3994.

[91] Arvind A, Kumar V, Saravanan P, Mohan CG. Homology modeling, molecular dynamics and inhibitor binding study on MurD ligase of Mycobacterium tuberculosis. Interdiscip Sci-Comput Life Sci 2012;4:223–38. http://dx.doi.org/10.1007/s12539-012-0133-x.

[92] Pratvielsosa F, Menginlecreulx D, Vanheijenoort J. Over-production, purification and properties of the uridine-diphosphate N-acetylmuramoyl-L-alanine-D-glutamate ligase from Escherichia-coli. Eur J Biochem 1991;202:1169–76. http://dx.doi.org/10.1111/j.1432-1033.1991.tb16486.x.

[93] Walsh AW, Falk PJ, Thanassi J, Discotto L, Pucci MJ, Ho HT. Comparison of the D-glutamate-adding enzymes from selected gram-positive and gram-negative bacteria. J Bacteriol 1999;181:5395–401.

[94] Bertrand JA, Auger G, Fanchon E, Martin L, Blanot D, vanHeijenoort J, Dideberg O. Crystal structure of UDP-N-acetylmuramoyl-L-alanine: D-glutamate ligase from Escherichia coli. Embo J 1997;16:3416–25. http://dx.doi.org/10.1093/emboj/16.12.3416.

[95] El Zoeiby A, Sanschagrin F, Levesque RC. Structure and function of the Mur enzymes: development of novel inhibitors. Mol Microbiol 2003;47:1–12. http://dx.doi.org/10.1046/j.1365-2958.2003.03289.x.

[96] Bertrand JA, Auger G, Martin L, Fanchon E, Blanot D, La Beller D, van Heijenoort J, Dideberg O. Determination of the MurD mechanism through crystallographic analysis of enzyme complexes. J Mol Biol 1999;289:579–90. http://dx.doi.org/10.1006/jmbi.1999.2800.

[97] Falk PJ, Ervin KM, Volk KS, Ho HT. Biochemical evidence for the formation of a covalent acyl-phosphate linkage between UDP-N-acetylmuramate and ATP in the Escherichia coli UDP-N-acetylmuramate:L-alanine lipase-catalyzed reaction. Biochemistry 1996;35:1417–22. http://dx.doi.org/10.1021/bi952078b.

[98] Crick DC, Mahapatra S, Brennan PJ. Biosynthesis of the arabinogalactan-peptidoglycan complex of Mycobacterium tuberculosis. Glycobiology 2001;11:107R–18R. http://dx.doi.org/10.1093/glycob/11.9.107R.

[99] White TA, Kell DB. Comparative genomic assessment of novel broad-spectrum targets for antibacterial drugs. Comp Funct Genomics 2004;5:304–27. http://dx.doi.org/10.1002/cfg.411.

[100] Zhang R, Ou HY, Zhang CT. DEG: a database of essential genes. Nucleic Acids Res 2004;32:D271–2. http://dx.doi.org/10.1093/nar/gkh024.

[101] Kotnik M, Humljan J, Contreras-Martel C, Oblak M, Kristan K, Herve M, Blanot D, Urleb U, Gobec S, Dessen A, Solmajer T. Structural and functional characterization of enantiomeric glutamic acid derivatives as potential transition state analogue inhibitors of MurD ligase. J Mol Biol 2007;370:107–15. http://dx.doi.org/10.1016/j.jmb.2007.04.048.

[102] Mengin-Lecreulx D, Falla T, Blanot D, van Heijenoort J, Adams DJ, Chopra I. Expression of the Staphylococcus aureus UDP-N-acetylmuramoyl-L-alanyl-D-glutamate : L-lysine ligase in Escherichia coli and effects on peptidoglycan biosynthesis and cell growth. J Bacteriol 1999;181:5909–14.

[103] Anwar RA, Vlaovic M. Udp-N-acetylmuramoyl-L-alanyl-D-glutamyl-L-lysine synthetase from Bacillus-sphaericus – activation by potassium phosphate. Biochem Cell Biol-Biochim Biol Cell 1986;64:297–303.

[104] Vollmer W, Blanot D, de Pedro MA. Peptidoglycan structure and architecture. FEMS Microbiol Rev 2008;32:149–67. http://dx.doi.org/10.1111/j.1574-6976.2007.00094.x.

[105] Michaud C, Menginlecreulx D, Vanheijenoort J, Blanot D. Over-production, purification and properties of the uridine-diphosphate-N-acetylmuramoyl-L-alanyl-D-glutamate – meso-2,6-diaminopimelate ligase from Escherichia-coli. Eur J Biochem 1990;194:853–61. http://dx.doi.org/10.1111/j.1432-1033.1990.tb19479.x.

[106] Mengin-Lecreulx D, Michaud C, Richaud C, Blanot D, Vanheijenoort J. Incorporation of Ll-diaminopimelic acid into peptidoglycan of Escherichia-Coli mutants lacking diaminopimelate epimerase encoded by Dapf. J Bacteriol 1988;170:2031–9.

[107] Auger G, van Heijenoort J, Vederas JC, Blanot D. Effect of analogues of diaminopimelic acid on the meso-diaminopimelate-adding enzyme from Escherichia coli. Febs Lett 1996;391:171–4. http://dx.doi.org/10.1016/0014-5793(96)00619-9.

[108] Boniface A. Etude des relations structure-activité au sein de la famille des Mur synthétases, enzymes de la voie de biosynthèse du peptidoglycane. Orsay, France: Université Paris-Sud; 2007.

[109] Hammes WP, Neukam R, Kandler O. Specificity of uridine diphospho-n-acetylmuramyl-alanyl-d-glutamic acid – diamino acid ligase of bifidobacterium-globosum. Arch Microbiol 1977;115:95–102. http://dx.doi.org/10.1007/bf00427851.

[110] Huber R, Langworthy TA, Konig H, Thomm M, Woese CR, Sleytr UB, Stetter KO. Thermotoga-Maritima sp-Nov represents a new genus of unique extremely thermophilic eubacteria growing up to 90-Degrees-C. Arch Microbiol 1986;144:324–33. http://dx.doi.org/10.1007/bf00409880.

[111] Boniface A, Bouhss A, Mengin-Lecreulx D, Blanot D. The MurE synthetase from Thermotoga maritima is endowed with an unusual D-lysine adding activity. J Biol Chem 2006;281:15680–6. http://dx.doi.org/10.1074/jbc.M506311200.
[112] Gordon E, Flouret B, Chantalat L, van Heijenoort J, Mengin-Lecreulx D, Dideberg O. Crystal structure of UDP-N-acetylmuramoyl-L-alanyl-D-glutamate: meso-diaminopimelate ligase from Escherichia coli. J Biol Chem 2001;276:10999–1006. http://dx.doi.org/10.1074/jbc.M009835200.
[113] Yan YW, Munshi S, Leiting B, Anderson MS, Chrzas J, Chen ZG. Crystal structure of Escherichia coli UDPMurNAc-tripeptide D-alanyl-D-alanine-adding enzyme (MurF) at 2.3 angstrom resolution. J Mol Biol 2000;304:435–45. http://dx.doi.org/10.1006/jmbi.2000.4215.
[114] Basavannacharya C, Moody PR, Munshi T, Cronin N, Keep NH, Bhakta S. Essential residues for the enzyme activity of ATP-dependent MurE ligase from Mycobacterium tuberculosis. Protein Cell 2010;1:1011–22. http://dx.doi.org/10.1007/s13238-010-0132-9.
[115] Anderson MS, Eveland SS, Onishi HR, Pompliano DL. Kinetic mechanism of the Escherichia coli UDPMurNAc-tripeptide D-alanyl-D-alanine-adding enzyme: use of a glutathione S-transferase fusion. Biochemistry 1996;35:16264–9. http://dx.doi.org/10.1021/bi961872.
[116] Longenecker KL, Stamper GF, Hajduk PJ, Fry EH, Jakob CG, Harlan JE, Edalji R, Bartley DM, Walter KA, Solomon LR, Holzman TF, Gu YG, Lerner CG, Beutel BA, Stoll VS. Structure of MurF from Streptococcus pneumoniae co-crystallized with a small molecule inhibitor exhibits interdomain closure. Protein Sci 2005;14:3039–47. http://dx.doi.org/10.1110/ps.051604805.
[117] Duncan K, Vanheijenoort J, Walsh CT. Purification and characterization of the D-alanyl-D-alanine-adding enzyme from Escherichia-coli. Biochemistry 1990;29:2379–86. http://dx.doi.org/10.1021/bi00461a023.
[118] Bugg TDH, Wright GD, Dutkamalen S, Arthur M, Courvalin P, Walsh CT. Molecular-basis for vancomycin resistance in Enterococcus-faecium Bm4147-biosynthesis of a depsipeptide peptidoglycan precursor by vancomycin resistance proteins Vanh and Vana. Biochemistry 1991;30:10408–15. http://dx.doi.org/10.1021/bi00107a007.
[119] Kollonit J, Barash L, Kahan FM, Kropp H. New antibacterial agent via photofluorination of a bacterial cell-wall constituent. Nature 1973;243:346–7. http://dx.doi.org/10.1038/243346a0.
[120] Duncan K, Vanheijenoort J, Walsh CT. Biochemistry 1990;29:2379.